Harnessing Microbial Interactions to Elicit the Production of Polyene Macrolides in *Streptomyces*

Master's thesis

University of Turku

Department of Biochemistry

Molecular Systems Biology

December 2018

Mitchell Laughlin

The originality of this thesis has been checked in accordance with the University of Turku quality assurance system using the Turnitin OriginalityCheck service.

UNIVERSITY OF TURKU

Department of Biochemistry

Laughlin, Mitchell: Harnessing Microbial Interactions to Elicit the Production of Polyene Macrolides in Streptomyces

Master's Thesis, 96 p.

Molecular Systems Biology

December 2018

Summary

Since their discovery in the 1950s, polyene macrolides have been invaluable for treating life threatening fungal infections. Polyene antibiotics are unique because they target ergosterol, the fungal sterol, and disrupt the cellular processes that rely on ergosterol to function. While drug resistance threatens the utility of all other antifungal drug classes, polyene resistant strains remain rare. However, the polyene antibiotics in use have severe, dose-limiting side effects, and survival rates for systemic fungal infections are low. New compounds with improved therapeutic efficacy are needed.

Polyene macrolides are produced by the soil bacteria *Streptomyces*. *Streptomyces* have an extensive and carefully regulated secondary metabolism which enables them to outcompete co-inhabiting microorganisms by producing antibiotics suited for the present stressor. Over two-thirds of the clinical antibiotics derived from a natural source are produced by *Streptomyces*, but there has been a marked regression in compound discovery in recent decades. The standardized use of cell monoculture techniques could be why the full production potential of *Streptomyces* is not met in a laboratory setting.

In the current work, four strains of *Streptomyces* were cultured with baker's yeast *Saccharomyces cerevisiae* to elicit the production of secondary metabolites that are not observed in monoculture conditions. One strain produced undecylprodigiosin and a cyclized derivative, but the other three strains produced significant amounts of unidentified polyene macrolides in co-culture conditions. Extracts from the *Streptomyces* were tested for bioactivity against yeast and analyzed with high pressure liquid chromatography, mass spectrometry and nuclear magnetic resonance.

Key words: polyene macrolide, *Streptomyces*, antifungal activity, prodigiosin

Contents:

Abbreviations

1D	one dimensional
2D	two dimensional
AmB	amphotericin B
amu	atomic mass unit
ATCC27952	*Streptomyces peucetius*
BGC	biosynthetic gene cluster
BKMA 840	*S. lavendulae*
^{13}C NMR	carbon-13 nuclear magnetic resonance
°C	degrees Celsius
$CaCO_3$	calcium carbonate
CFU	colony forming units
COSY	correlation spectroscopy
DNA	deoxyribose nucleic acid
DOPC	1,2-di-oleoylphosphatidylcholine
ERG2	C-8 sterol isomerase
ERG3	C-5 sterol desaturase
ERG6	C-24 sterol methyltransferase
ERG11	lanosterol 14a-demethylase
$FeSO_4 \cdot 7\ H_2O$	iron sulfate heptahydrate
g	gram
g	gravitational force
g/L	grams per liter
HMBC	heteronuclear multiple-bond correlation spectroscopy
^{1}H NMR	proton nuclear magnetic resonance
H_2O	di-hydrogen monoxide
HPLC	high pressure liquid chromatography
hrs	hours

Hsp90	heat shock protein 90
HSQC-de	depth edit heteronuclear single-quantum correlation spectroscopy
ISP4	international *Streptomyces* project inorganic salt starch agar 4
JCM 4712	*S. hygroscopicus*
K_2HPO_4	dipotassium hydrogen phosphate
KNO_3	potassium nitrate
L	liter
LC-MS	liquid chromatography mass spectrometry
MeOH	methanol
$MgSO_4$	magnesium sulfate
MIC	minimal inhibitory concentration
mL	milli-liter
$MnCl_2 \cdot 4\ H_2O$	manganese(II) chloride tetrahydrate
MS	mass spectrometry
NaCl	sodium chloride
NH_4NO_3	ammonium nitrate
$(NH4)_2SO_4$	ammonium sulfate
nm	nanometer
NMR	nuclear magnetic resonance
PKS	polyketide synthase
RED2	metacycloprodigiosin
RED3	undecylprodigiosin
ROS	reactive oxygen species
t1PKS	type 1 polyketide synthase
TLC	thin layer chromatography
uv/vis	ultraviolet—visible spectroscopy
µl	microliter
YPD	yeast extract peptone dextrose medium
$ZnSO_4 \cdot 7\ H_2O$	zinc sulfate heptahydrate

1 Literature Review

1.1 Streptomyces: Natural Chemists

Streptomyces is a genus of mycelial, soil-dwelling actinobacteria that is best known for producing a diverse abundance of biologically active metabolites. Compounds produced by *Streptomyces* include hydrolytic exoenzymes and an array of structurally complex antibiotics. Hydrolytic exoenzymes facilitate decomposition in soil by freeing carbon from organic debris that cannot dissolve in water. The digested debris from plant cellulose and fungal chitin then serve as nutrient sources for *Streptomyces* and other competing microbes in the microenvironment. (Barka et al., 2016) When nutrients become limited, antibiotics are produced to give a competitive advantage over neighboring species (Netzker et al., 2018). As soil nutrients deplete, mycelial structures lyse to release the intracellular nutrients needed to produce spores. *Streptomyces* will remain dormant in spores until growth conditions improve. To protect the nutrients released from lysed mycelial cells during sporulation, antibiotics are essential. (Traxler & Roberto, 2015)

The antibiotics produced by *Streptomyces* belong to a class of metabolic products known as secondary metabolites; these compounds are not required for cells to develop and reproduce (Scherlach et al., 2013). Secondary metabolites improve survivability of *Streptomyces*, and a vast amount have been developed as anticancer drugs, antifungal drugs, pesticides and clinical antibiotics for human use (Medema et al., 2014). Two-thirds of all naturally derived antibiotics in use have been developed from *Streptomyces (*Barka et al., 2016). However, the full production potential of secondary metabolites is not reached when *Streptomyces* are grown under standard laboratory conditions. Genome sequencing reveals a multitude of biosynthetic gene clusters (BGC) that remain silent in laboratory cultivations. (Wezel & McDowall, 2011)

For decades, *Streptomyces coelicolor* has served as a model species for studying antibiotic biosynthesis and regulation, and it was revered for producing four clinically significant antibiotics (Challis, 2014). The true production potential of *S. coelicolor* was first noticed in 2002 when the full genome sequence was published, and 7,825 genes were predicted. The genome contains more than 20 BGCs which encode the enzymes needed to synthesize as many individual secondary metabolites. The sequence also predicted 965 regulatory proteins and 65 sigma factors responsible for controlling secondary metabolite biosynthesis. (Bentley et al., 2002) Further genome analysis of other species of *Streptomyces* has revealed even greater potential; some species could produce more than 50 different secondary metabolites if they are grown in suitable conditions. (van der Meij et al., 2017)

1.2 Polyene Macrolides, Generally

Polyene macrolides are a class of bioactive polyketides primarily produced by streptomycetes and other actinobacteria (Caffrey et al., 2016). These compounds have between 20 and 40 carbons and contain three distinct chemical regions on a macrolactone ring. All polyene macrolides have a polar polyhydroxylated region and a strongly non-polar chromophore region containing three to eight carbon—carbon double bonds in conjugation. Many polyenes have a deoxy amino sugar residue attached by a glycosidic bond, as well as various carbonyl and hemiketal domains on the macrocyclic structure. The deoxyaminosugar and a carboxylic acid group make up the polar head of these compounds. (Kong et al., 2013)

1.2.1 Polyene Biosynthesis

The biosynthesis of all polyenes follows a similar scheme (Figure 1). The backbone of the macrolactone aglycone is assembled by modular type 1 polyketide synthase (t1PKS) enzymes composed of distinct domains. The acyl transferase domain selectively binds

small carboxylic acid units and transfers them to the ketosynthase domain. Decarboxylative condensation reactions add the building blocks to the growing chain that is held to the PKS enzyme by an acyl carrier protein. The selectivity of the acyl transferase for chain building units provides a factor of structural diversity between PKSs. The possible presence of ketoreductase, dehydratase or enoyl reductase modules in the PKS creates further diversity. An absence of these domains results in a fully oxidized ketones in the chain, whereas activity of all three results in the fully reduced saturated bonds. Hydroxyl groups and double bonds are formed in the presence of ketoreductase and ketoreductase with dehydratase, respectively. (Hopwood, 1997; Zotchev, 2003; Kong et al., 2013)

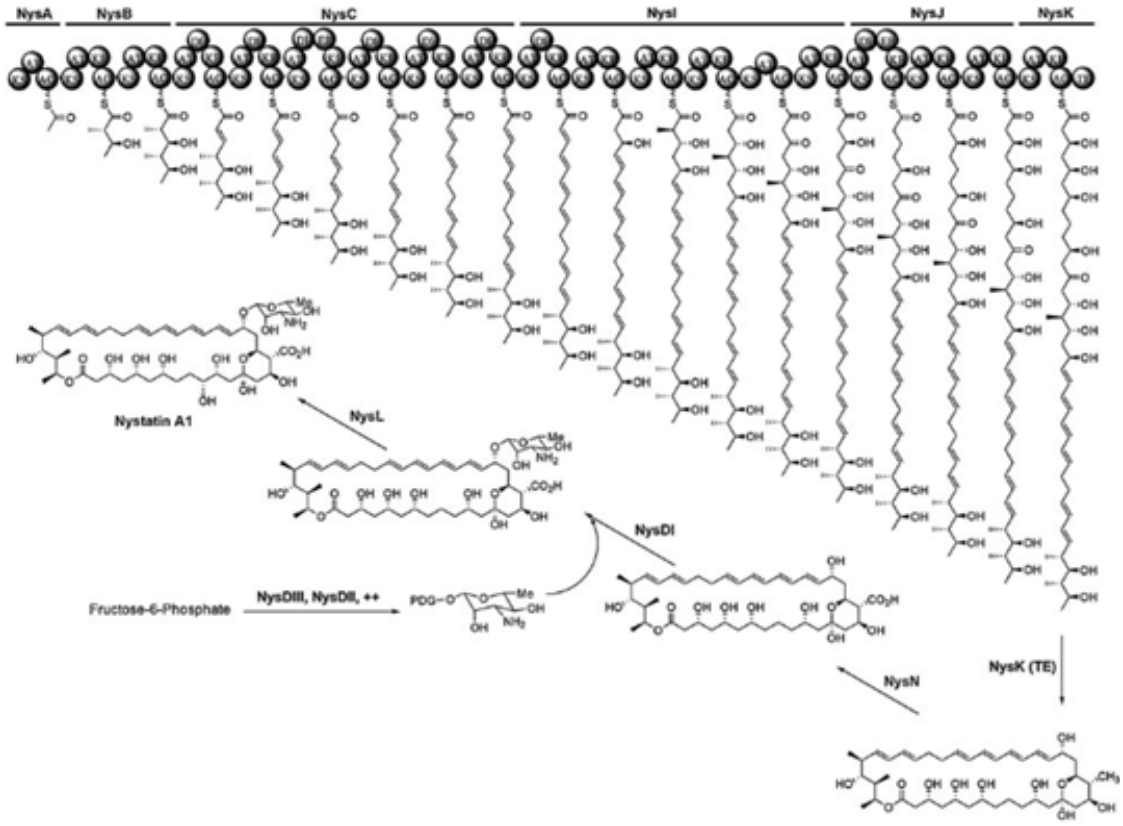

Figure 1: The biosynthesis of nystatin (Kong et al., 2013).

Ultimately, the chain is cleaved from the acyl carrier protein, and a thioesterase domain cyclizes the chain. After the cyclization, a glycosyltransferase adds a sugar residue to the

first carbon after the chromophore region. An exocyclic methyl group on the fourth carbon after the chromophore is oxidized to a carboxyl group by cytochrome P450. The exocyclic carboxyl group and amino sugar are invaluable to the antifungal activity of polyenes, and positioning relative to the chromophore is largely conserved. (Aparicio et al., 2003) Some polyenes may undergo additional glycosylation reactions, or the exocyclic carboxyl group may convert to a carboxamide. The polyol chain can be further modified by cytochrome P450 to add more hydroxyl groups, or a hemiketal ring may form through the action of additional monooxygenases. The breadth of the structural diversity of polyenes grows as they continue to be studied. (Caffrey et al., 2016; Low et al., 2018)

1.2.2 Classifications and Properties of Polyene Macrolides

Polyenes are classified as glycosylated or non-glycosylated, based on the presence of a sugar residue, and as trienes, tetraenes, pentaenes, hexaenes, heptaenes or octaenes, depending on the size of the chromophore. Compounds that have sp^3 hybridized carbons within the chromophore are termed "degenerated," since the conjugated system is disrupted by saturated bonds. (Zotchev, 2003) Degenerated polyenes have slightly lower antifungal activity than polyenes with intact chromophores. (Aszalos et al., 1985) The conjugated system of the chromophore distinguishes polyenes from other classes of macrolides and attributes identifying chemical properties. (Zotchev, 2003)

The uv/vis absorption spectra of polyenes have three distinct peaks that shift to longer wavelengths as the size of the chromophore increases (Figure 2). For example, the tetraenes, nystatin and natamycin, and the pentaene filipin appear brownish-yellow, while heptaenes, like amphotericin B, appear dark yellow (Thomas, 1976). The chromophore is responsible for the interaction between polyenes and ergosterol, which is the primary fungal cell membrane sterol. Through the affinity of the chromophore towards ergosterol, polyene antibiotics invade the cell membrane. This interaction is

essential to the antimycotic properties of these antibiotics. (Ciesielski et al., 2016) Polyenes with more conjugated double bonds have greater affinity towards ergosterol than cholesterol and, therefore, higher biological activity and lower toxicity (Aszalos et al., 1985). However, polyenes with larger chromophores are more hydrophobic, which limits their dissemination throughout the aqueous portions of body (Thomas, 1976).

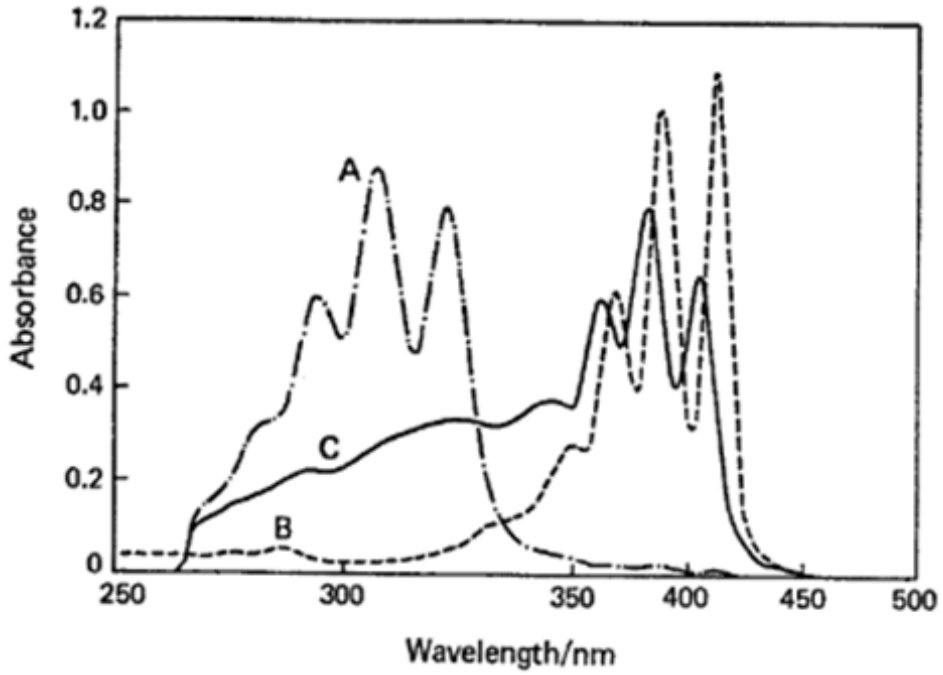

Figure 2: Spectra of a tetraene (A) and two heptaenes (B and C) (Thomas, 1976).

Polyenes have comparably poor solubility in organic solvents due to the hydrophilic polyhydroxylated region or polyol chain. The polyol chain is located opposite to the chromophore on the macrolactone ring and may contain an epoxide group, carbonyl groups, and several hydroxyl groups. Carboxylic acid is generally one of the carbonyl groups; it exists as a zwitterion if the polyene possesses an amino sugar. (Thomas, 1976; Hamill, 2013) The amino sugar is usually mycosamine, but it can be perosamine. Sugars are linked to the carbon adjacent to the chromophore three carbons away from the carboxylic acid. Only glycosylated polyenes are in clinical use, since the polar nature of

the amino sugar group greatly improves solubility in water and the affinity of the drugs for ergosterol over cholesterol. (Zotchev, 2003; Kong et al., 2013)

1.3 Polyene Antibiotics in Clinical Use

While over 200 unique polyene macrolides with antifungal activity have been isolated from *Streptomyces* and other actinomycetes since the first was discovered in 1950, only a fraction are suitable for clinical use (Figure 3) (Zotchev et al., 2003). Polyene macrolides are among the most toxic compounds used in modern medicine; lethal side effects often limit dosage and therapy duration (Janout et al., 2015). Poor solubility *in vivo* causes drug toxicity and greatly limits drug dispersal to all niches of the body. Intravenous administration is necessary for treatment of systemic fungal infections, but oral and topical administration are effective for treatment of superficial thrush. (Santos-Aberturas et al., 2015; Lyu et al., 2016)

Polyene antibiotics have a broad spectrum of activity toward fungi, and a mechanism of action that is refractory to the evolution of resistance. They are the only class of antifungals to act from the cell exterior by directly targeting membrane sterols. Rates of acquired resistance remain low after decades of monotherapy treatments. (Kong et al., 2013; Vincent et al., 2013) Polyenes will remain an indispensable therapeutic option. Resistance to all other classes of antifungal drugs arises soon after they are introduced into clinical practice. (Cannon et al., 2007; Walker et al., 2010) Nevertheless, there is great demand for polyenes with improved therapeutic activity, greater *in vivo* solubility and reduced toxicity (Cao et al., 2012). The most commonly used and well studied polyene macrolides include amphotericin B (AmB), nystatin, natamycin (pimaricin) and filipin III (Figures 3 and 4) (Caffrey et al., 2016).

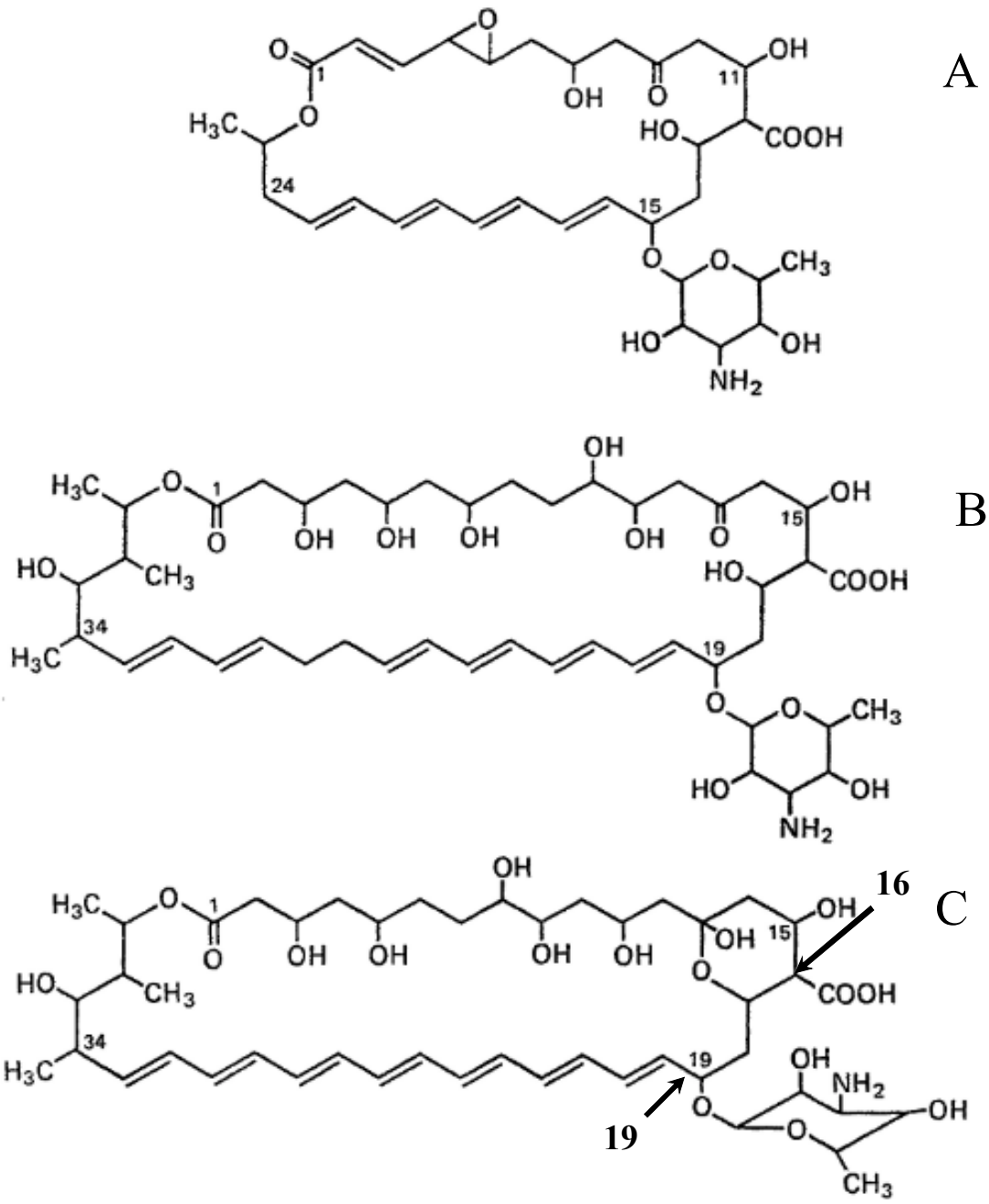

Figure 3: Structures of glycosylated polyene macrolides natamycin (A), nystatin (B) and amphotericin B (C). Figure altered from Thomas (1976).

1.3.1 Amphotericin B

Amphotericin B (AmB) (Figure 3C) was first isolated from *Streptomyces nodosus* in 1950 and was named for its amphoteric nature. It has been considered the gold standard

for treating life threatening systemic fungal infections since 1957. (Gupte et al., 2002) It is a glycosylated heptaene and the third most used antifungal drug (Vincent et al., 2013). AmB has been used as a model for studying polyenes, as it remains the only polyene macrolide suited for effective treatment of deep-seated fungal infections. The drug has potent antifungal activity, it is broad spectrum and active against fungi which have developed resistance to other clinical drugs. Often, AmB becomes the last treatment option for systemic mycoses. (Baginski et al., 2005; Malayeri et al., 2018) It is the only treatment option during pregnancy because it is not teratogenic (Johnson et al., 2018).

Despite clinical use world-wide as a monotherapy, resistance to AmB remains rare, and resistant strains do not persist. The decreased fitness and virulence of AmB-resistant fungi causes them to be outcompeted by native strains once antibiotic stress is removed. (Gray et al., 2012; Vincent et al., 2013) However, systemic fungal infections are still a serious health concern because AmB dosage and treatment duration are limited by equally concerning side effects (Wasko et al., 2012). Nephrotoxicity is the most cited concern, but there is also evidence that AmB alters the cellular composition of the blood, as anemia, thrombocytopenia and agranulocytosis follow AmB therapy. Side effects are primarily caused by the formation of drug aggregates *in vivo* which do not have the same selective toxicity as AmB monomers. The continued use of AmB makes apparent the lack of efficacious alternatives. (Lemke et al., 2005; Janout et al., 2015)

1.3.2 Nystatin

Nystatin (Figure 3B), initially called fungicidin, was discovered in 1950 from *Streptomyces noursei* (Hazen & Brown, 1950). It is a glycosylated polyene closely related to AmB, but it is classified as a tetraene or a degenerated heptaene because the chromophore is interrupted by a saturated bond (Romero et al., 2009). Nystatin has fungicidal activity against species of *Candida, Aspergillus*, *Histoplasma* and *Coccidioides,* including isolates resistant to AmB. However, its poor aqueous solubility

and formation of nonselective toxic aggregates *in vivo* preclude its use as a treatment for systemic mycoses. (Malayeri et al., 2018)

Nystatin is applied as a cream or used as a mouth wash to treat superficial infections, or it is administered orally to treat gastrointestinal infections. In these applications, nystatin does not have side effects, since extreme hydrophobicity prevents absorption though the skin or gastrointestinal tract. Immunocompromised patients undergoing radiation therapy or chemotherapy at high risk of opportunity fungal infection are often prescribed nystatin as a prophylactic. The drug prevents *Candida* from adhering to epithelial cells. Despite widespread use, there are no reported cases of resistance to nystatin. (Scheibler et al., 2017)

1.3.3 Natamycin

Natamycin (Figure 3A), or pimaricin, is a small-sized glycosylated tetraene first isolated in 1955 from *Streptomyces natalensis* (Malayeri et al., 2018). The fungicidal potency and small size of this drug relative to other polyenes provoked extensive investigation into its mechanism of action, which has improved understanding of the function of all polyenes (te Welscher et al., 2008).

Natamycin is both colorless and odorless and is therefore an ideal preservative to inhibit fungal growth in cheeses, sausages, yogurts and wines. It has been used in the food industry for over thirty years. The surface treatment of cheeses and sausages with natamycin is considered safe, since ultraviolet light degrades natamycin on the products by the time of consumption. Similar to other polyenes, natamycin is too hydrophobic to be absorbed through the gastrointestinal lining, so there is small risk of side effects. However, there is mounting concern that continual consumption of the drug in yogurts and wines will give rise to polyene-resistant fungi. (Paseiro-Cerrato et al., 2013; Dalhoff & Levy, 2015)

Medically, natamycin is most prominently used as eyedrops to treat ophthalmic mycoses. It is most effective against infections caused by *Aspergillus* or *Fusarium*, and it is the primary treatment for fungal keratitis. (Aparicio et al., 2016) Natamycin is also used as a cream to cure topical infections caused by a great variety of fungi and some protozoa (Ciesielski et al., 2016).

1.3.4 Filipin

Filipin (Figure 4) is a complex of uncharged pentaenes with strong antifungal properties; it is produced by various strains of *Streptomyces* (Caffrey et al., 2008). Upon interaction with a cell membrane, filipin forms large complexes with sterols in the hydrophobic membrane interior and causes gross fragmentation. Unlike most known polyenes, it is non-glycosylated and shows similar affinity toward both cholesterol and ergosterol. (Zotchev, 2003; te Welscher et al., 2008)

Filipin is too toxic to be used in human therapy because it is not sufficiently selective for ergosterol containing membranes. Instead, it is used as a means to determine the cholesterol content of membranes and as a reference for studies on the biosynthesis and activity of other polyene macrolides. It is used clinically to diagnose some metabolic disorders. Filipin is produced as four related variants, known as the filipin complex. Each variant in the filipin complex differs in the number of hydroxyl functional groups present. Filipin III is the major product. Filipin II is the second most prevalent, and it is a biosynthetic precursor to filipin III. (Payero et al., 2015)

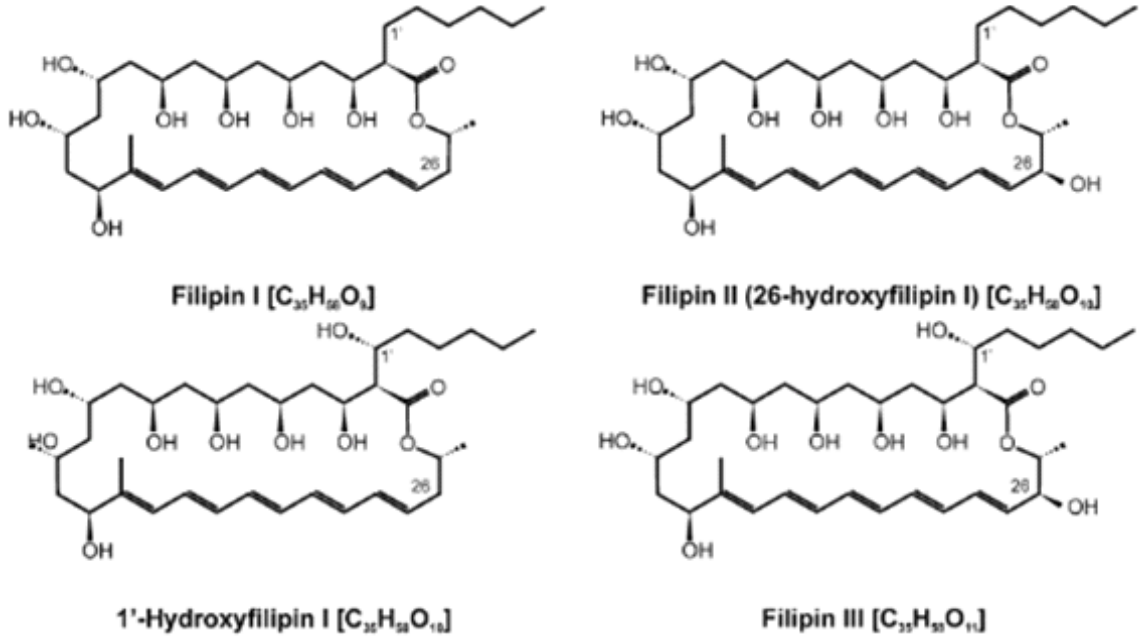

Figure 4: The structures of the compounds in the filipin complex. Filipin III is the final major product in the complex. Figure altered from Payero et al., 2015.

1.4 Antifungal Activity of Polyene Antibiotics

Glycosylated polyene macrolides have multiple antifungal modes of action, which have been investigated since the discovery of the compounds in the 1950s. All of the known mechanisms involve an interaction between polyenes and ergosterol molecules in either the fungal cell membrane or the mitochondrial membrane. (Caffrey et al., 2016) The various details and effects of the interactions are not completely understood, but what has been elucidated will be discussed in coming section.

Some polyene macrolides form ion pores in the cellular membrane through complex associations with membrane sterols to cause leakage of cell components, while others aggregate on the membrane surface to sequester ergosterol and disrupt ergosterol dependent cell processes (Caffrey et al., 2016). A more recent series of research points to the ability of polyene macrolides to induce oxidative damage in fungal cells through action at the mitochondrial membrane (Sangalli-Leite et al., 2011; Mesa-Arango et al., 2014; Shekova et al., 2017). Regardless, fungal cell death caused by polyenes is a long-

term, multistage event where interconnected pathways shut down due to an interaction of the drugs with ergosterol (Chudzik et al., 2015).

1.4.1 Membrane Permeabilization

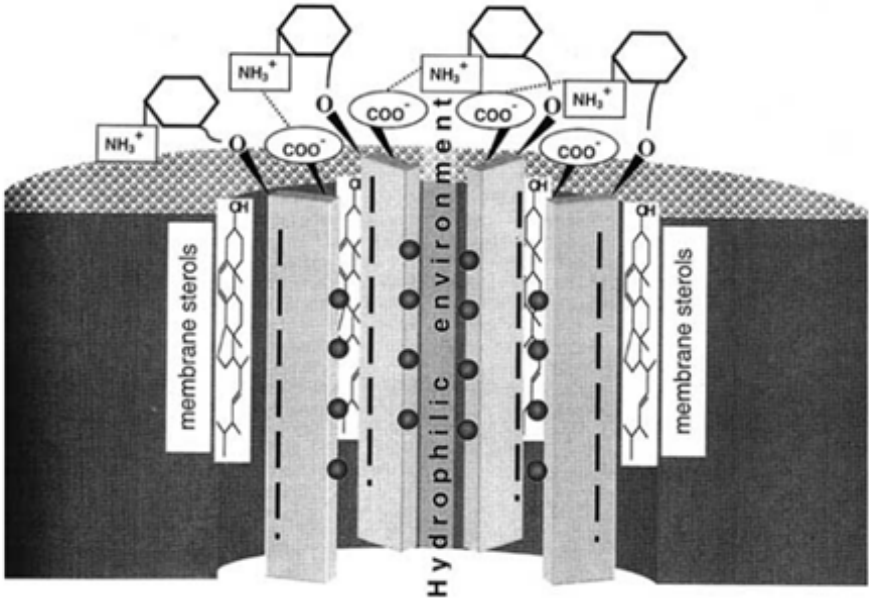

Figure 5: Cross-section of the transmembrane pore formed by amphotericin B in a fungal cell membrane. The polyol and chromophore regions are represented by the spheres and dashes, respectively (Zotchev, 2003).

Permeabilization of the fungal cell membrane is the earliest and most well known model of polyene macrolide activity. In this model, 3 to 17 polyene molecules bind to an equal amount of ergosterol molecules to form hydrophilic pores in the cell membrane. For AmB, the pore is a complex of eight AmB molecules stacked with eight ergosterol to form a barrel. The AmB is oriented with the hydrophobic chromophores facing outwards towards the fatty-acid tails of the membrane and the hydrophilic polyol chains facing the interior (Figure 5). (Zotchev, 2003; Janout et al., 2015) The hydrophilic nature of the pore interior allows intracellular ions, such as K^+, Na^+ and Mg^{2+}, to efflux to the hypotonic cell exterior. The electric potential that is created across the membrane by the efflux of the cations then causes hydrogen atoms to influx through the same pores.

Increasing the concentration of H^+ results in acidification and eventual precipitation of components of the fungal cell cytoplasm. (Hamill, 2013)

1.4.2 Formation of the Membrane Pore

The formation and stability of the membrane pores formed by polyene macrolides have been studied using AmB as a model drug. Dimers and larger aggregates of AmB form in aqueous solutions at any pH via hydrophobic interactions between the chromophores. It is suspected that AmB molecules orient antiparallel to one another in intermolecular interactions because aggregate formation is not inhibited in basic aqueous solutions. At pH 12, the amino sugar protonates and the molecular charge becomes neutral. Electrostatic repulsion between the anionic carboxylic acid groups would otherwise inhibit aggregate formation in basic solutions. (Wasko et al., 2012) The aggregates resulting from the limited solubility of polyenes in water are important for eventual membrane pore formation, since many AmB molecules must be in the same location to form a membrane spanning pore (Zotchev, 2003; Tutaj et al., 2015).

Dimers and aggregates of AmB initially attach to the fungal cell membrane via hydrogen bond formation between the amino groups of the mycosamine sugars and the phosphate groups of the membrane phospholipids. The AmB aggregates are perpendicular to the membrane surface with their chromophores interacting and their polyol regions facing outwards. This initial binding event will occur even if the membrane does not contain sterols. Further hydrogen bonding, between the outward facing polyol regions and the membrane phospholipid phosphate groups, pull apart the hydrophobic interactions between the chromophores. The exposed chromophores subsequently interact with the membrane phospholipid fatty acids and penetrate the outer surface of the cell membrane. (Zotchev, 2003; Romero et al., 2009; Cohen, 2010)

The polyol regions of the AmB molecules face toward each other and away from the cell interior in a V-shaped bowl. The hydrophobic ends of the molecules are held together via hydrogen bonding between the C35 hydroxyl groups. Membrane fluidity eventually causes the chromophore regions exposed to the membrane interior to interact with ergosterol or another sterol. Interaction with a sterol is essential for pulling the AmB molecules into the membrane to form a barrel, rather than a pocket. If no sterols are present in the membrane, the AmB pockets persist because of the low free energy at the membrane surface. (Romero et al., 2009; Cohen et al., 2010)

After the AmB pocket forms a barrel perpendicular the membrane, the polar side of the macrolactone ring, which contains the carboxylic acid on C16 and the mycosamine sugar residue on C19, remains at the membrane surface (Figure 3C). The polyol regions of the AmB molecules in the complex interact with each other and form a hydrated pore. Hydrogen bonding between the carboxylic acid groups on C16 and the amino sugars on C19 of neighboring AmB molecules stabilize the pore. The membrane sterols in the complex fit between the AmB molecules in the barrel and interact with them via van der Waals forces. (Hartsel et al., 1993; Szpilman et al., 2008) Non-glycosylated polyenes can also form membrane pores, but pores without the stabilizing hydrogen bond between the carboxylic acid and amino sugar tend to be larger and less stable. Membrane fragmentation is common with non-glycosylated polyenes. (Zotchev, 2003)

1.4.3 Proposed Amphotericin B Pore Conformations

The length of an AmB molecule is 21Å, but cellular membranes are 43Å thick on average. This discrepancy has caused debate as to how AmB spans the entire membrane (Szpilman et al., 2008). Two models regarding how the pore spans the membrane have been proposed (Figure 6). In the first model, the membrane is pinched at the site of the pore, and a single barrel of AmB molecules spans the dimpled membrane. The C35 hydroxyl groups are thought to maintain the dimple by hydrogen bonding with the

phosphate groups on the inner side of the cell membrane. (Gray et al., 2012) The presence of ergosterol and the hydrogen bonding between the polar heads of AmB and membrane phospholipids are important for stabilizing the membrane dimple in the single barrel model (Romero et al., 2009; Cohen 2010).

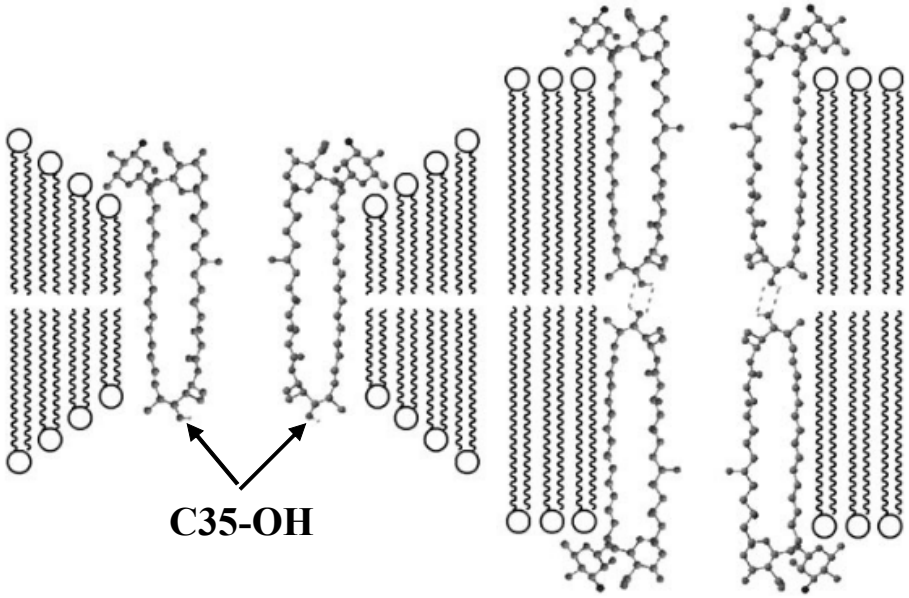

Figure 6: Single-barrel and double-barrel models of the amphotericin B pore. Hydrogen bonding between C35 -OH groups is indicated with dotted lines. The figure is altered from Szpilman et al. (2008).

The double barrel pore model (Figure 6) is made up of two AmB barrel complexes linked tail-to-tail by hydrogen bonds between the C35 hydroxyl groups. The polar regions of the AmB barrels face the inner and outer membrane surfaces. (Szpilman et al., 2008; Gray et al., 2012) The double barrel model is supported by studies that have demonstrated that AmB has maximum ion conductance only when the drug is present on both sides of the membrane (Hartsel et al., 1993).

The mechanism by which the inner membrane layer pore forms is not well understood, since the polar region of AmB should not cross the hydrophobic membrane interior by passive diffusion. It is hypothesized that membrane disruption caused by polyene aggregates at the membrane's outer surface could push some polyenes entirely into the

membrane's interior. Repulsion between the polar region of AmB and the membrane interior could result in some AmB molecules oriented with the polar heads on the inner membrane surface. Channel formation would occur as it did on the outer membrane surface. The channels starting from opposite sides of the membranes would eventually connect through hydrogen bonding between the C35 hydroxyl groups. (Hartsel et al., 1993; Zotchev, 2003) Regardless of the pore model, the C35 hydroxyl group has been proven to be crucial for the formation of membrane spanning pores. AmB analogs with a methyl group at C35 instead of a hydroxyl group were unable to form electrolyte conducting channels in liposomes. (Szpilman et al., 2008)

1.4.4 Types of Amphotericin B Pores

Two different types of AmB membrane permeabilizing structures, called non-aqueous channels and aqueous pores (Figure 7), form depending on: the concentration of AmB, the availability of ergosterol and the prevalence of cholesterol in the cell membrane. The substrate specificities and contributions to cell death differ for the two structures. At first, non-aqueous channels, that do not include ergosterol, form. They are permeable to monovalent cations during short-lived open states, but impermeable to monovalent anions. Aqueous pores form when the AmB molecules in non-aqueous channels bind to ergosterol in the cell membrane. Stabilization from the sterols allows aqueous pores to span the entire membrane. Aqueous pores require more AmB and ergosterol to form, since AmB molecules must be in complex with ergosterol on each side of the membrane. The pores accommodate glucose, large electrolytes and monovalent anions and cations. (Cohen et al., 2010; Mesa-Arango et al., 2012)

Pore formation occurs in milliseconds, but it is delayed in membranes containing only cholesterol (Mesa-Arango et al., 2012). The threshold concentration of AmB that must be reached for aqueous pores to form is mainly determined by the presence of ergosterol or cholesterol in the lipid membrane. Sterols are required to stabilize the membrane

spanning pore. Non-aqueous channels form at AmB concentrations of 0.05 x 10^{-6} M and 0.5 x 10^{-6} M in membranes containing only ergosterol or only cholesterol, respectively. Aqueous channels form when AmB reaches concentrations of 0.4 x 10^{-6} M in membranes containing only ergosterol and 1.6–2.9 x 10^{-6} M in membranes containing only cholesterol. (Mouri et al., 2008) A greater concentration of AmB is required to form aqueous pores because the double-barrel pore model requires AmB on the intracellular membrane surface (Tutaj et al., 2015).

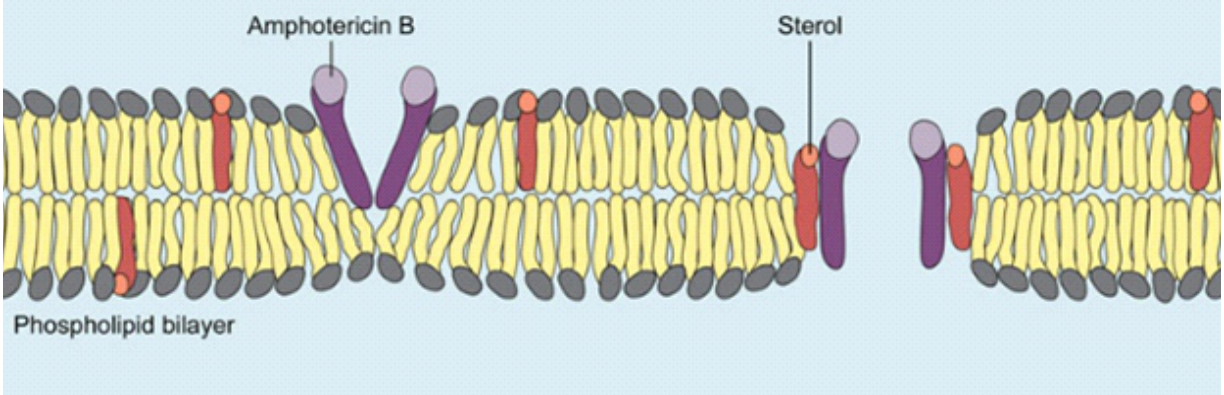

Figure 7: Non-aqueous channel (left) and aqueous pore (right). Aqueous pores form when non-aqueous channels complex with ergosterol. The aqueous pore is represented by a single-barrel model (Cohen, 2010).

Permeability kinetics studies on the two membrane pore types were conducted by preparing liposomes from fungal cell plasma membranes. The liposomes were suspended in hyper-osmotic solutions of either urea or a nitrate salt. The effects of increasing AmB concentrations on liposome swelling were observed to determine whether the solutes were able to enter the liposomes through the AmB pores. At lesser concentrations of AmB, liposome swelling occurred only in the nitrate salt solution. Swelling was only observed in the urea solution after AmB reached a threshold concentration and aqueous pores formed. (Cohen 2010)

It has been proven by using the K^+ channel blocking compound tetraethylamonium (TEA), that the size of the AmB membrane channel increases with increasing AmB

concentration. TEA is a 4Å molecule, and ion permeability through non-aqueous channels is completely blocked by TEA until a threshold concentration of AmB is reached and aqueous pores can form. TEA is unable to block ion permeability through aqueous pores. These results suggest that the AmB aqueous pore has a diameter between 4.5Å and 5Å. (Cohen, 2010)

1.4.5 The Sequestration of Ergosterol

Ergosterol sequestration (Figure 8) is a more recently accepted mechanism of polyene antifungal activity, and it was proven to be the primary fungicidal mechanism of action for AmB and natamycin (te Welscher et al., 2008; Palacios et al., 2011; Gray et al., 2012; Anderson et al., 2014). Polyenes sitting on the outer surface of the cell membrane sequester ergosterol at the membrane surface. The drug-sterol complex either exists as a single layer or as large aggregates. These conformations, respectively, are the surface adsorption model and sterol sponge model of ergosterol sequestration. The overall decrease in ergosterol concentration within the cell disrupts processes that require ergosterol. Intracellular enzymes and membrane transporters need ergosterol to solubilize; alternative sterols are not effective replacements and cause additional stress to the cell. (Mesa-Arango et al., 2012; Caffrey et al., 2016) Additional effects of ergosterol sequestration are discussed in section 1.4.8. Ion channel formation is an important mechanism for polyene macrolide antibiotics, but it has been shown to be complementary to the effects of ergosterol sequestration (Gray et al., 2012).

Membrane permeabilization and cell death are not always related. Filipin and natamycin cause minimal membrane leakage before cell death, while polyenes fungi-chromin and rimocidin incite strong K^+ efflux, but are weakly fungicidal. Nystatin causes greater K^+ efflux but is less cytotoxic than both AmB and an AmB methyl ester derivative. (Chen et al., 1978) The C16 carboxylic acid group in AmB methyl ester is converted to an ester, so the derivative cannot support membrane pores. AmB methyl ester is as cytotoxic as

native AmB at, but it has a slower killing rate than native AmB. (Gary-Bobo, 1989) The comparable toxicities of the membrane permeabilizing native AmB and non-permeabilizing AmB methyl-ester suggest that membrane pore formation is a secondary mechanism for fungal cell death (Chen et al., 1978).

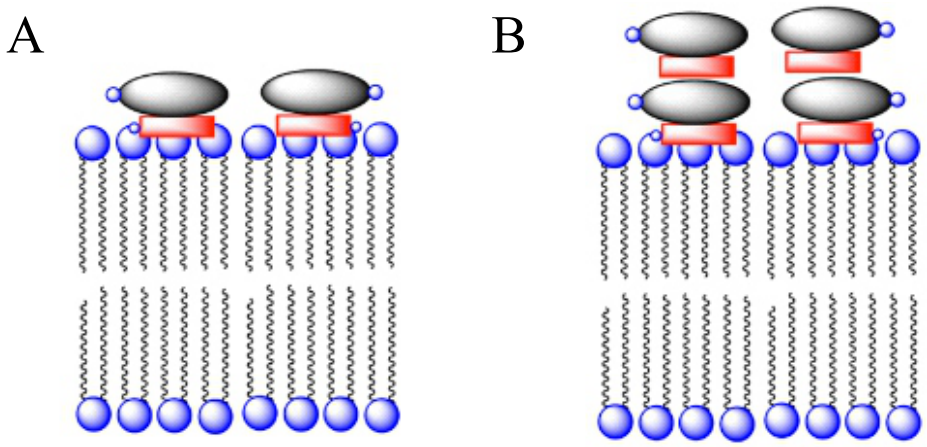

Figure 8: Surface adsorption (A) and Sterol Sponge (B) models of AmB ergosterol sequestration. AmB (grey) extracts ergosterol (red) from cells and sequesters it as the membrane surface as a single layer or as large aggregates (Janout et al., 2015).

1.4.6 Mycosamine in Ergosterol Sequestration

Gray et al. (2012) investigated the functional groups necessary for AmB to have antifungal activity. AmB derivatives with both the C35 hydroxyl group removed and the C16 carboxylic acid group changed to a methyl ester were tested for antifungal activity (Figure 9). Membrane pores were not formed by derivatives lacking the C35 hydroxyl group because intermolecular hydrogen bonds between C35 hydroxyl groups are critical for the formation of the AmB double barrel pore. The hydrogen bond from the C16 carboxylic acid group also plays a role in pore stabilization, as well as in initial contact with membrane phosphate groups. Membrane pores were not possible as an antifungal mechanism with either of these derivatives. (Zotchev 2003; Szpilman et al., 2008; Gray et al., 2012)

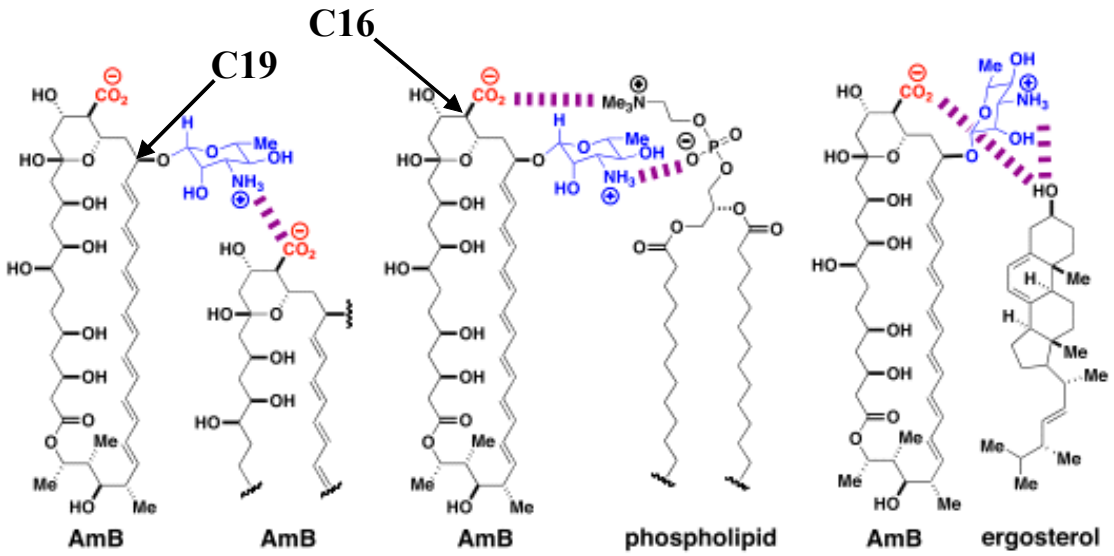

Figure 9: Hydrogen bonding of the C16 carboxylic acid group (red) and C19 mycosamine group (blue) on AmB with another AmB molecule, a membrane phospholipid and ergosterol. The figure is altered from Palacios et al. (2011).

However, the non-permeabilizing AmB derivatives maintained potent antifungal activity. The mycosamine residue was unaltered in the derivatives and binding to ergosterol was not inhibited. Only derivatives with the C19 mycosamine sugar residue removed lacked antifungal activity. (Gray et al., 2012) The amino group on the mycosamine sugar plays a role in the initial hydrogen bonding between AmB and the phosphate groups on the cell membrane surface. The sugar residue also promotes the extraction of sterols from the membrane via hydrogen bonding between its amino group and the hydroxyl group on ergosterol. In addition, the amino group on the sugar residue stabilizes the membrane pore through hydrogen bonding with the C16 carboxylic acid group. (Palacios et al., 2011)

1.4.7 The Sterol Sponge

Anderson et al. (2014) demonstrated that the sterol sponge is the primary form of the AmB-ergosterol complex and the main mode of action for AmB (Figure 8B). Solid state NMR was used to confirm that the majority of AmB does not reside within the cell

membrane. Transmission electron microscopy images confirmed the NMR results; large aggregates of AmB and ergosterol were observed on the imaged membranes soon after AmB was added. (Anderson et al., 2014) It was confirmed that the extra-membranous aggregates extract ergosterol from the membrane by using imbedded spin labels to detect ergosterol in the membrane interior. Before AmB was added to the membranes, ergosterol NMR signals were shifted by the spin label probes within the membrane bilayer, but ergosterol signals were not shifted by the probes after AmB was added. Therefore, ergosterol occupies a position on the membrane surface when AmB is present. An *in vivo* test with yeast cells demonstrated that AmB that is pre-saturated with ergosterol is not cytotoxic to cells, even though the aggregates bound to living cells. (Anderson et al., 2014)

1.4.8 Ergosterol Sequestration by Natamycin

Evidence that the cytotoxic activity of polyenes does not rely on membrane permeabilization caused interest in the mechanisms of small polyenes. Natamycin, a small polyene, was initially hypothesized to have a mode of action unrelated to ergosterol, since it is unable to form pores. However, natamycin was the first polyene proven to kill yeast solely by binding to ergosterol. (te Welscher et al., 2008) Non-permeabilizing AmB derivatives have antifungal activity comparable to that of natamycin (Gray et al., 2012). More natamycin binds to membranes containing ergosterol than membranes containing cholesterol. The minimal inhibitory concentration (MIC) of natamycin increases 15-fold against yeast engineered to primarily synthesize cholesterol. However, at no concentration does natamycin cause cation efflux *in vivo* or *in vitro.* (te Welscher et al., 2008)

Natamycin sequesters ergosterol at the membrane surface by directly binding to it. However, large extracellular drug-sterol aggregates do not form (Figure 8A). In a subsequent study, te Welscher et al. (2010) investigated the effects of natamycin on the

membrane fission and fusion events in vacuolar transport. These dynamic events require membranes to reorganize into highly curved intermediate forms, stabilized by ergosterol (Burger, 2000). A saturating amount of natamycin inhibited 71% of vacuole fusion. Filipin and nystatin are more potent at saturating concentrations because, in addition to binding ergosterol, they cause membrane lysis. A staging assay determined that natamycin inhibits vacuole fusion at the priming phase when the membrane curve must be supported by ergosterol. (Peters et al., 2001; te Welscher et al., 2010)

A later study by te Welscher et al. (2012) proved that the action of natamycin on ergosterol inhibits cell growth by stalling membrane transport proteins for amino acids and glucose. Membrane composition changes when ergosterol is sequestered, and transmembrane proteins become insoluble. Amino acid transport was blocked in a model fungi after incubation with natamycin. Glucose transport was also completely inhibited, but eventually recovered. Transcriptome analysis showed that the transporters were up-regulated in a natamycin dose-dependent manner. However, only glucose transport recovered because expression of the sugar transporters was more than double that of the amino acid transporters. How quickly membrane transport resumes after natamycin stress is removed depends on the solubilities and expression levels of transport proteins. (Mesa-Arango et al., 2012; te Welscher et al., 2012)

1.4.9 Induction of Oxidative Damage

Sangalli-Leite et al. (2011) evaluated the effects of AmB on the encapsulated yeast *Cryptococcus neoformans*. Two cell viability tests provided paradoxical results. After incubation with AmB, no *C. neoformans* cells survived even though the cell membranes were intact. In a parallel XTT assay, which measures cell metabolism through the reduction of an indicator salt, more reduction occurred at higher concentrations of AmB. The results suggested that AmB induces oxidative damage to the cell cytoplasm without forming membrane pores. Further assays revealed that at MIC concentrations of AmB,

intracellular free radicals are produced and protein carbonylation occurs. (Sangalli-Leiti et al., 2011) The induction of oxidative damage subsequently causes cells to undergo apoptosis. Mature fungal biofilms are cleared *in vivo* by AmB induced apoptosis (Delattin et al., 2014).

Cells treated with free radical scavengers before the addition of AmB show less evidence of intracellular oxidative damage (Mesa-Arango et al., 2012). It was proposed that AmB itself induces oxidation via the putative redox activity of the heptaene chromophore moiety (Hartsel et al., 1993; Sangalli-Leiti et al., 2011). This mechanism was disproven using synthetic AmB derivatives that were unable to bind ergosterol, but readily associated with lipid bilayers. Even though the heptaene chromophore was intact, the derivatives lacked antifungal activity. (Palacios et al., 2011)

How AmB causes oxidative damage was investigated in multiple strains of pathogenic fungi. Reactive oxygen species (ROS) are natural byproducts of mitochondrial respiration, and they are required for AmB to cause oxidative damage. To lessen mitochondrial ROS content, rotenone, a toxin found in plants, was used to inhibit complex I of the electron transport chain. Fungal strains treated with rotenone before AmB treatment did not experience oxidative bursts and had significantly improved survivability. (Mesa-Arango et al., 2014) AmB causes extensive lipid oxidation at the mitochondria, which suggests that the oxidative burst occurs through disruption of the ergosterol containing mitochondrial membrane (Shekova et al., 2017).

1.4.10 Oxidative Damage in Resistant Fungi

The production of ROS and the oxidative burst were evaluated in AmB resistant fungi to understand the intracellular source of the radical species. ROS were not present in AmB resistant strains after treatment with the drug, and it was proposed that resistant strains produce fewer ROS. AmB resistant strains use alternative electron transfer and oxygen

reduction mechanisms that consume less molecular oxygen. Inhibition of the alternative oxidase decreased oxygen consumption in AmB resistant strains by more than 90%, indicating reliance on the alternative electron transfer mechanism. AmB resistant strains produce fewer ROS, and thereby lessen oxidative damage caused by lysis of the mitochondrial membrane. (Mesa-Arango et al., 2014; Shekova et al., 2017)

The constitutive activity of heat shock protein 90 (Hsp90) in AmB resistant fungi further inhibits the oxidative burst. Hsp90 promotes a variety of stress response pathways, including antioxidant mechanisms. AmB resistant fungi use alternative sterols to which AmB cannot bind. However, the disruption of the ergosterol synthesis pathway produces ROS, as pathway intermediates accumulate and hazardous side reactions produce alternative sterols. (Vincent et al., 2013) There is no opportunity for a damaging oxidative burst when the stress response pathway is constitutively active. Catalase, a ROS-detoxifying enzyme, is continually expressed with 2.5 times greater frequency in AmB resistant fungi. (Mesa-Arango et al., 2014)

1.5 Interactions & Toxicity of Polyenes

Polyene macrolides can be used therapeutically to treat systemic fungal infections because they have a higher binding affinity with the ergosterol found in fungi than the cholesterol found in human cells (Zotchev, 2003; Umegawa et al., 2011). The toxicity of polyene antibiotics is mainly attributed to unwanted interactions with cholesterol. Although it has been shown that pore formation in membranes containing cholesterol requires higher concentrations of polyenes, toxicity still occurs *in vivo* due to the prevalence of polyene aggregates. (Mesa-Arango et al., 2012)

The low aqueous solubility of polyenes causes them to aggregate through hydrophobic interactions between chromophores. High localized concentrations of polyenes lose selectivity for fungal pathogens; the drug aggregates are equally damaging towards host

cells. (Caffrey et al., 2016) Lysis of red blood cells by polyene aggregates, and the resulting anemia, is a major source of toxicity (Ciesielski et al., 2016). However, nephrotoxicity, which occurs as polyenes are filtered out of the blood by the kidneys, is the main dose-limiting side-effect that often requires antibiotic courses to be ended prematurely (Caffrey et al., 2008; Hamill 2013).

1.5.1 Cholesterol and Ergosterol

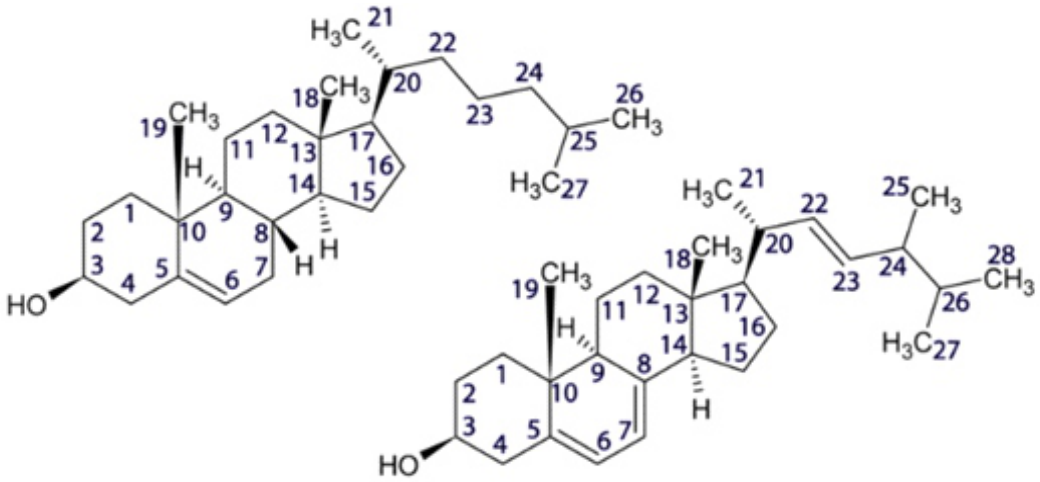

Figure 10: Structures of cholesterol (left) and ergosterol (right) (Ciesielski et al., 2016).

Cholesterol and ergosterol have only minor structural differences, which contribute to polyene selectivity for fungal membranes (Figure 10). Ergosterol has one additional double bond in the second ring, between carbons 7 and 8, and one in the tail chain, between carbons 22 and 23. The additional pi-bonds make the molecule more elongated and rigid than cholesterol. The greater rigidity and flatness of ergosterol allows for more stable electrostatic interactions with polyenes, and the two additional pi-bonds offer more opportunities for pi-stacking interactions with the polyene chromophore. (Hartsel et al., 1993; Umegawa et al., 2011)

The differences in interaction strength between a polyene and ergosterol and a polyene and cholesterol is minor when single molecules are considered. However, multiple

polyene molecules must bind many sterols from a single cell to be cytotoxic. A cumulative effect from multiple polyene-sterol interactions results in polyene selective toxicity for fungal cells. Rates of sterol sponge and membrane pore formation are slower in cholesterol containing membranes. Single polyene molecules may bind cholesterol containing membranes transiently during treatment, but it is unlikely that enough AmB would bind to kill the effected human cell. (Baginski et al., 2002; Mouri et al., 2008) The use of alternative sterols, which are structurally similar to ergosterol, by AmB resistant strains corroborates the importance of minor structural differences in sterols with regard to polyene toxicity (te Welscher et al., 2008; Caffrey et al., 2016). However, this explanation of drug selectivity is only true when polyenes exist as single molecules in solution. Aggregates of polyenes are not selective for ergosterol.

1.5.2 Attempts to Reduce Polyene Toxicity

For polyene selectivity to persist *in vivo*, aggregate formation must be prevented (Szlinder-Richert et al., 2001). Containing AmB in liposomes allows for the gradual release of ergosterol-selective monomers. Lipid-based drug delivery systems have been shown to significantly reduce nephrotoxicity and improve survivability of AmB treatment by 28%. (Lemke et al., 2005) However, for regular treatments, these lipid formulations remain too expensive to manufacture (Caffrey et al., 2016).

Semi-synthetic polyenes offer further opportunities to reduce toxicity. AmB molecules with the C16 carboxylic acid group converted to an ester are significantly less able to permeabilize cholesterol containing membranes than ergosterol containing membranes. An anionic carboxylic acid group stabilizes the positively charged mycosamine moiety in an orientation favorable for hydrogen bond formation with a sterol. (Gary-Bobo, 1989)

AmB derivatives with a large molecular umbrella attached to the C16 carboxylic acid group are unable to form aggregates and retain antifungal activity comparable to the native drug (Figure 11). These derivatives do not form pores, and rely on the surface adsorption mechanism. Hemolytic activity and mammalian cytotoxicity were minimized in tests with the umbrella formulation. (Janout et al., 2015) Multiple other semi-synthetic derivatives of AmB and other polyenes have been attempted, but they are often too difficult to synthesize for clinical application to be feasible. As a result, AmB has remained the only polyene suitable for systemic treatment without viable alternatives over the last 50 years. (Hamill, 2013; Caffrey et al., 2016)

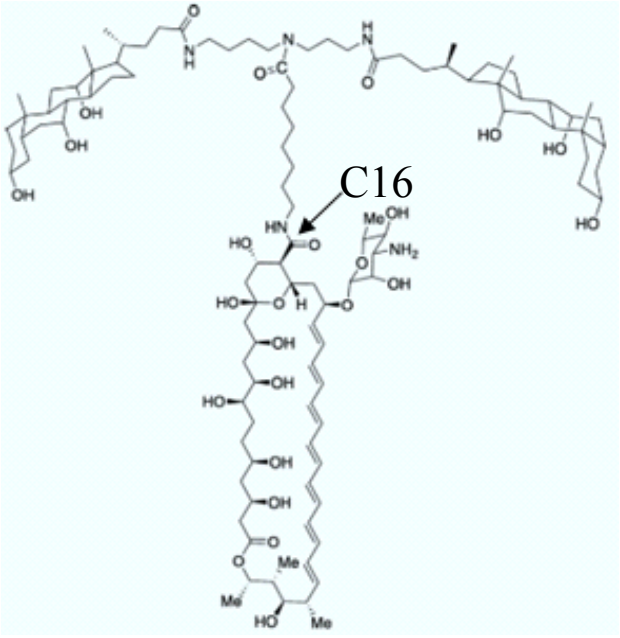

Figure 11: Structure of an umbrella-tamed amphotericin B molecule formulated by Janout et al., 2015. The umbrella is attached to the C16 carboxylic acid group and prevents formation of molecular aggregates in aqueous solution. (Janout et al., 2015)

1.5.3

Polyene Interactions with Membranes

A clear understanding of the interactions between polyenes and sterols is needed to guide the development of semi-synthetic polyene formulations. Solid state NMR is used to determine the relative binding affinities of polyenes for membrane components.

Synthetic 1,2-di-oleoylphosphatidylcholine (DOPC) membranes that contain either ergosterol or cholesterol are incubated with either AmB or natamycin. Then, the attenuated NMR signals from the polyene-bound DOPC and sterols are compared to determine the relative binding affinities of polyenes for the membrane components. AmB preferentially interacts with ergosterol over DOPC in ergosterol containing liposomes. However, AmB has equal affinity toward cholesterol and DOPC in liposomes prepared with cholesterol. (Janout et al., 2015; Ciesielski et al., 2016)

Synthetic membranes containing ergosterol more readily absorb AmB than cholesterol containing membranes (Kamiński et al., 2014). AmB profoundly affects membrane dynamics and the NMR signals of all membrane sterols and lipids. Carbon signals from the lipid chain tail region are particularly altered. This indicates that AmB inserts into the membrane. Natamycin, in contrast, specifically affects ergosterol and does not influence membrane dynamics or insert into the membrane. Natamycin also interacts with cholesterol, but interaction with DOPC is not apparent. (Ciesielski et al., 2016)

1.5.4 Polyene Interactions with Sterols

Comparisons between NMR spectra of membrane sterols in the presence and absence of polyenes enables assignment of the sterol carbons with which AmB and natamycin interact. In cholesterol, AmB causes signal attenuation mainly from carbons in the first and forth rings, but not in methyl groups 18 and 19 which are outside the plane of the core ring system (Figure 10). The exclusion of the non-planar methyl carbons and core rigidity of cholesterol in the presence of AmB suggests a planar interaction. Apart from the terminal carbons, the flexible tail region of cholesterol is unaffected by AmB. Natamycin has similar interactions with cholesterol in the first and forth rings. However, natamycin does interact with methyl groups 18 and 19, so it must bind to the other face of cholesterol. (Ciesielski et al., 2016)

AmB engages ergosterol along the ring structure and primarily dampens signals at the ridges between rings (Figure 12). A non-planar methyl group is engaged, indicating that AmB binds ergosterol on the side opposite to which it binds cholesterol. The ergosterol tail region is immobilized by the interaction, but the terminal chain carbons are not bound. The additional double bond in the ergosterol tail makes it more planar and better suited to bind to the rigid AmB structure. (Ciesielski et al., 2016)

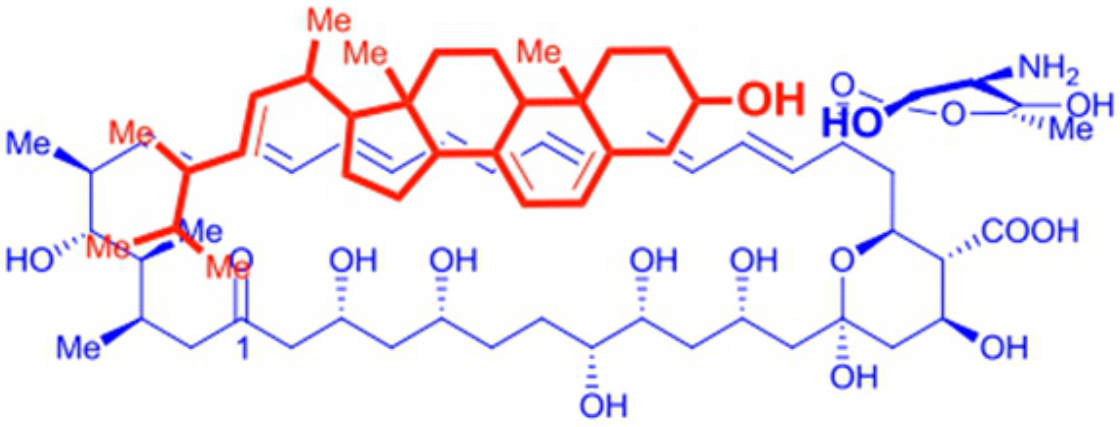

Figure 12: The head-to-head interaction between AmB (blue) and ergosterol (red). (Ibrahim, 2013)

A study on the orientation of the AmB-ergosterol complex confirmed that both head-to-head and head-to-tail interactions occur between the two molecules. The head region in ergosterol has the hydroxyl group, and the head region in AmB contains the carboxylic acid and mycosamine residues. Head-to-head interactions between the polar regions occur more frequently. Head-to-tail interactions exist when ergosterol is in complex with many AmB molecules. In either pairing, the tail of ergosterol is in an extended conformation. (Umegawa et al., 2011)

Natamycin attenuates far more ergosterol signals than it does cholesterol signals, including the terminal chain carbons which are forced to a position unfavorable for the tail (Ciesielski et al., 2016). The observed strong natamycin-ergosterol interactions explain the low toxicity of the drug in clinical use (Wang et al., 2018).

1.6 Microbial Resistance to Polyene Macrolides

1.6.1 Treatment Options for Infectious Fungi

Candida albicans is an opportunistic fungal pathogen with infection severity ranging from superficial thrush to invasive systemic mycoses. People with compromised immune systems as a result of cancer treatment, human immunodeficiency virus, or the immunosuppressive drugs that are given during organ transplants, are especially susceptible. (Sanglard et al., 2003) *C. albicans* is the most prevalent infectious fungi for humans and the fourth most common pathogen infecting hospital patients. Mild and life threatening systemic infections are initially treated with broad spectrum triazoles and echinocandin drugs, respectively. However, *de novo* resistance to triazoles arises frequently, and resistance to echinocandins is becoming more prevalent. (Walker et al., 2010) If a systemic infection becomes resistant to both of these drug types, amphotericin B is the final treatment option (Vincent et al., 2013).

Despite severe nephrotoxicity, poor solubility *in vivo*, and patient mortality rates of nearly 50%, AmB has been vital for treating systemic mycoses for over 50 years. It remains the third most used antifungal drug because fungal resistance arises extremely rarely in both clinical and laboratory settings. Theoretically, AmB resistant strains should be more common, since dose-limiting renal toxicity prevents complete regimens of AmB monotherapy, and poor penetration of AmB to all niches of the body fosters environments where resistance could evolve *in vivo*. (Thomas 1976; Anderson et al., 2014; Caffrey et al., 2016)

Analysis of 9,252 clinically isolated *Candida* species revealed that 99.8% were sensitive to AmB. It is rare for the utility of a widely used antibiotic to persist for so long. 5-flucytosine was used for less than 20 years before it became obsolete, and the frequency of echinocandin resistance is steadily rising after just 17 years of clinical use. (Pfaller et al., 2012) The development of fungal resistance to nystatin is also rare, but systemic use

of the compound is not possible due to toxicity. The rarity of nystatin resistance is even more perplexing, as it is widely used as a long-term prophylactic topical agent for infants and immunocompromised patients (Gupte et al., 2002)

1.6.2 Resisting Antifungal Drugs

A study by Vincent et al. (2013) sought to elucidate why resistance to polyenes, and AmB specifically, is so rare. The group acquired AmB-resistant strains of *C. albicans* isolated from clinics and engineered resistant strains. The genomes of the resistant strains were sequenced to determine the mutations that confer AmB resistance; the ergosterol biosynthetic pathway was specifically considered. *C. albicans* clinical isolates most commonly resisted AmB via a double loss of function in *ERG3* and *ERG11*, or by loss of function in either *ERG2* or *ERG6*. (Sanglard et al., 2003; Vincent et al., 2013)

ERG2, ERG3, ERG6 and *ERG11* are the most relevant antifungal drug targets in the ergosterol biosynthetic pathway. These enzymes catalyze the tailoring reactions that convert lanosterol to ergosterol. Inhibiting any of the pathway enzymes prevents ergosterol biosynthesis and causes toxic sterol intermediates to accumulate. However, strains that resist the enzyme-targeting antifungal drugs are common. (Ghannoum & Rice, 1999; Sanglard et al., 2003) Minor mutations to the drug binding sites in the ergosterol biosynthetic enzymes confer resistance against antifungal drugs that target these enzymes by preventing drug binding. The minor mutations allow ergosterol biosynthesis to continue, and ergosterol is the functional sterol in strains resistant to the enzyme-targeting antifungal drugs. The inactivation of the tailoring enzymes to prevent ergosterol production is required in AmB resistant *C. albicans* mutants. The lack of ergosterol necessitates the use of alternative sterols, such as lanosterol, to which AmB cannot bind. (Anderson et al., 2014; Zhou et al., 2018) The hazards to fungi which resist polyene macrolides by stalling ergosterol biosynthesis are further explored in the following section.

1.6.3 Fitness Costs of Alternative Sterols in Resistant Strains

Lanosterol is the first precursor in the ergosterol biosynthetic pathway after the cyclization of the common sterol precursor, squalene (Sanglard et al., 2003). While the use of lanosterol allows *C. albicans* to resist drugs that target ergosterol, there are significant costs to fitness because of the structural differences between lanosterol and ergosterol. Proteins in the membrane and cytoplasm rely on ergosterol to support proper structure and function. Lanosterol is an ineffective replacement; sterol-dependent proteins have reduced activity in AmB resistant strains of *C. albicans*. Pathogenicity is hampered in strains relying on lanosterol, and these strains are quickly cleared by the host's immune system, should resistant strains arise *in vivo.* (Anderson et al., 2014)

ERG3 and *ERG11* double knockout mutants of *C. albicans* are avirulent in a mouse model and are unable to cause damage to human epithelial cells *in vitro*. While tissue invasion by the double knockout mutants is comparable to wild-type, the production of inflammatory cytokines and the presence of reactive oxygen species are greatly reduced. The *ERG11* knockout mutants have increased sensitivity to reactive oxygen species. (Vincent et al., 2013; Zhou et al., 2018)

Strains of *C. albicans* lacking ERG11 activity are unable to survive in aerobic environments unless ERG3 is also suppressed. This phenomenon is likely caused by additional stress from the disrupted ergosterol biosynthetic pathway. Since ERG11 is the first enzyme to act on lanosterol in wild-type fungi, lanosterol accumulates when ERG11 is inhibited. At elevated concentrations of lanosterol, other enzymes in the ergosterol pathway convert lanosterol to alternative sterols. (Sanglard et al., 2003) The activity of the other pathway enzymes causes toxic sterol intermediates and ROS to accumulate. Cell growth is slowed due to metabolic capacity being consumed by the constitutive activation of stress response pathways. (Cannon et al., 2007)

As mentioned in section 1.4.10, the abundance of toxic sterol intermediates and ROS make AmB resistant mutants dependent on Hsp90, which promotes stress response pathways. Hsp90 can be down regulated by 10-fold after stress in wild-type *C. albicans* to liberate cell resources for other processes. However, constitutive Hsp90 expression is necessary in AmB resistant strains, even in the absence of stressors from drugs or the host immune system. AmB resistant strains treated with Hsp90 inhibitors did not grow *in vitro*, and *de novo* emergence of resistant mutants was prevented by partially inhibiting Hsp90 function. (Vincent et al., 2013)

The extreme dependence on Hsp90 activity creates possibilities for effective combination therapies using AmB and Hsp90 inhibitors. Combination therapies could reduce the required dosage of AmB and help to mitigate its severe toxicity, which has caused patient survival rates to remain near 50%. (Vincent et al., 2013) Development of this kind of combination therapy is important because virulent AmB resistant fungi could evolve. Fungi from the genus *Penicillium* produce and resist AmB without any effects on cell viability. Horizontal gene transfer from AmB producing strains to pathogenic fungi could give rise to polyene resistance that does not impact cell fitness (Svahn et al., 2015)

Disruption of the ergosterol biosynthesis pathway is a detrimental strategy for fungi to resist polyene antibiotics. The inefficiency of sterol-dependent proteins and the prevalence of toxic sterol intermediates when *C. albicans* depends on lanosterol cause resistant strains to be outcompeted when selective pressure is removed. The constant activity of stress response pathways consumes cell resources and limits adaptability to adverse conditions; immunocompromised patients are able to survive AmB resistant *C. albicans* because the mutants are hypersensitive to fever. (Vincent et al., 2013)

Other strategies of antibiotic resistance are not applicable to polyenes because they directly target the cell membrane via an interaction with ergosterol. This is paramount to

the continued utility of polyene antibiotics (Kong et al., 2013). The other drug targets in *C. albicans* are enzymes involve in RNA synthesis, ergosterol biosynthesis and cell wall biosynthesis. Enzyme targeting drugs can be resisted without dramatic cost to the cell. Drugs with intracellular targets can be resisted by increased expression of drug efflux pumps, destroying the drug, or over-expressing the drug target. The drug binding site on an enzyme can be mutated to prevent drug action without impeding enzyme activity. These resistance mechanisms do not hamper cell survivability and persist when antibiotic stress is removed. Drug destroying enzymes and efflux pumps can be regulated as needed, and enzymes with point mutations continue to be used. (Cannon et al., 2007)

It is imperative for the continued utility of antibiotics that drug mechanisms of action are refractory to the evolution of antibiotic resistance. If resistance does arise, it should consume significant cell energy so that resistant strains are outcompeted by drug sensitive strains when stress is removed. Presently, polyene macrolides are the only class of antifungal drug to give rise to unstable resistant strains. (Vincent et al., 2013)

1.7 Finding New Polyenes

Streptomyces are collected from a diversity of biomes in the search for undiscovered compounds. A marked regression in the discovery of new compounds began in the 1980s, and it has lead the search to increasingly remote and extreme environments, ranging from antarctic soils to tropical anthills. (Svahn et al., 2015; Van Arnam et al., 2016) To determine if a species produces any compounds with medically advantageous bioactivity, a *Streptomyces* isolate is grown in different conditions, and culture extracts are screened for secondary metabolites (Liu et al., 2013).

If a potentially interesting compound is found, the genome of the isolate is sequenced and exploited to improve production of the discovered compound. However, many

BGCs remain silent when *Streptomyces* are screened using standard laboratory methods because nutrient rich monocultures do not reflect the biological stresses of the natural environment. In the soil, innumerable microbes compete for limited resources; *Streptomyces* combat microbial competition via tightly regulated production of cytotoxic secondary metabolites. (Wezel & McDowall, 2011) Recent studies have shown that some BGCs may be switched on only when interspecies competition is introduced to laboratory culture conditions. Introducing microbial competition to *Streptomyces* cultivations may unveil new production potential in previously isolated strains. (Stubbendieck & Straight, 2016)

A study by Nazari et al. (2013) analyzed changes in the gene expression of *S. coelicolor* when it was grown on agar or in soil cultures with and without chitin as a carbon source. Chitin is the second-most abundant polysaccharide by biomass in nature and is a major component of the fungal cell wall. The expression of 675 genes was significantly changed by the addition of chitin to cell cultures, and eight BGCs were induced. The gene cluster most prominently up-regulated in response to the chitin was a cryptic t1PKS; polyenes are one possible product from unidentified t1PKS gene clusters. (Nazari et al., 2013) *Streptomyces* are well adapted to regulate secondary metabolism in response to co-inhabiting competitors. Identifying how *Streptomyces* sense competition and regulate secondary metabolites can guide drug discovery when genetic information is available (Mendes et al., 2007).

To date, all gene clusters encoding the enzymes that produce small-sized polyenes are known to contain a cholesterol oxidase encoding gene. The cholesterol oxidase enzyme serves as a fungal sensor and triggers antifungal production (Cao et al., 2012; Payero et al., 2015; Aparicio et al., 2016). Cholesterol oxidase catalyzes the first step in the degradation of natural sterols including cholesterol and ergosterol. In *S. natalensis*, cholesterol oxidase is required for the biosynthesis of natamycin. The location of the cholesterol oxidase gene, *pimE,* in the center of the natamycin gene cluster is indicative

of its role in natamycin production, but *pimE* is not a biosynthetic enzyme. Natamycin is not produced when *pimE* is knocked out, and production is restored by gene complementation or addition of PimE extract to knockout mutant cultures. Addition of cholesterol oxidases from different species to *pimE* knockout cultures also restores natamycin production. This indicates that the activity of cholesterol oxidase on a fungal cell component is involved in the function of the enzyme as a fungal sensor and positive regulator for the production of small-sized polyenes. (Antón et al., 2004; Mendes et al., 2007; Aparicio & Martin, 2008)

1.8 Introduction to the Current Work

There is constant demand for new antibiotics with better selectivity and reduced toxicity. The three most used polyene macrolide antibiotics were all first used in the 1950s. While polyene resistant fungi continue to be rare, the primary polyenes in use are not ideal drugs. (Vincent et al., 2013) Only AmB is suitable for systemic treatment of deep-seated mycoses, and its severe side-effects limit treatment success (Zotchev, 2003). Attempts to reduce the toxicity of existing polyenes by producing synthetic derivatives or developing slow-releasing formulations have been successful, but such approaches are too expensive or technically complicated for industrial scale production (Falk et al., 1999; Lemke et al., 2005; Hamill, 2013). It is therefore sensible to continue searching for polyene antibiotics in natural sources. Most antibiotics were initially discovered by screening actinomycetes isolated from soil in the 1950s; this discovery platform has been nearly exhausted. Only the most obscure natural sources are likely to yield strains that produce novel compounds. (Lewis, 2013)

However, a majority of *Streptomyces* screened in the past were grown in nutrient rich monocultures. Without the interspecies exchange of chemical signals, many BSGs would have remained silent during screening. Consequently, known strains have the potential to produce new compounds if the correct stimuli are introduced to cultures.

(Netzker et al., 2018) Genomic analysis determines which strains of *Streptomyces* should be further investigated using co-culture conditions (Bachmann et al., 2014). The search for new polyenes is guided by the knowledge that these compounds are produced by t1PKS gene clusters that contain a cholesterol oxidase gene. The cholesterol oxidase acts as a fungal sensor and enhances polyene production when fungi are present. (Aparicio et al., 2016)

In the current work, four strains of *Streptomyces* were cultured with autoclaved baker's yeast *Saccharomyces cerevisiae* to activate gene clusters predicted to produce polyenes. Crude extracts from the co-cultures were screened for polyenes using HPLC and MS. Three of the strains in the study were selected from the in-house strain collection based on available genome sequences. These strains each have a t1PKS cluster that contains a cholesterol oxidase.

The forth *Streptomyces* studied, REDMBK6, was a soil isolate from a university laboratory course. The isolate produces two red compounds, RED2 and RED3, in transfer media only when it is grown with whole autoclaved yeast cells; yeast extract does not elicit production in transfer media. The compounds were produced in other media whether whole yeast was present or not. The red compounds were purified, and their structures were solved using NMR. Genome sequencing aided in identifying the two red compounds as metacycloprodigiosin and undecylprodigiosin. MS and NMR results verified the identity of the compounds. Compound extracts have antifungal activity against yeast, and the production profile of the REDMBK6 strain changes depending on the nitrogen source provided.

2 Aims:

- Analyze the genomes in the in-house strain collection, and select *Streptomyces* with t1PKS gene clusters that contain a cholesterol oxidase encoding gene.
- Determine the production conditions of the red compounds produced by the laboratory course isolate *Streptomyces* strain REDMBK6.
- Grow the selected in house *Streptomyces* strains and REDMBK6 in media containing autoclaved whole yeast or yeast extract and compare the production profiles of the different cultivations using HPLC and MS.
- Elucidate the chemical structures of the compounds produced only in the presence of whole yeast using NMR.

3 Material & Methods

3.1 Strain Selection and Genome Mining

The uncharacterized *Streptomyces sp.,* REDMBK6, was isolated during a laboratory course and observed to produce red compounds. The strain was provided from the in-house strain collection.

The in-house *Streptomyces* genome collection was analyzed with Artemis genome browser (Carver et al., 2012) and AntiSMASH 4.1.0 (Blin et al., 2017) to identify strains that had t1PKS clusters containing cholesterol oxidase encoding genes. The strains selected for further investigation of polyene production were *S. hygroscopicus* JCM 4712, *S. peucetius* ATCC 27952 and *S. lavendulae* BKMA 840.

3.2 Cell Culturing and Production of Compounds

REDMBK6 cultivations were either started with 250 µl of mycelia cell preparations stored in 20% glycerol at -80°C, or with spores produced on ISP4 plates (10 g/L starch, 1.0 g/L K_2HPO_4, 1.0 g/L $MgSO_4$ x 7 H_2O, 1.0 g/L NaCl, 2.0 g/L $(NH4)_2SO_4$, 1.0 mL trace salt solution, 1.0 L distilled water. Trace salt solution contains 0.1 g $FeSO_4$ • 7 H_2O, 0.1 g $MnCl_2$ • 4 H_2O, and 0.1 g $ZnSO_4$ • 7 H_2O in 100 mL of distilled water.

REDMBK6 was grown in 250 mL Erlenmeyer flasks containing 25 mL media at 30°C with vigorous shaking for 3–5 days, depending on when the culture turned red. Transfer Media (10 g/L glucose, 1 g/L yeast or yeast extract, 1 g/L KNO_3, 0.1 g/L K_2HPO_4) was initially used to investigate the influence of yeast on production. The yeast was store bought baker's yeast, *Saccharomyces cerevisiae*. Russian yeast media (26 g/L whole yeast, 9 g/L glucose, 2 g/L $CaCO_3$, 2 g/L NH_4NO_3, 1 L tap water) was subsequently used to investigate the influence of different nitrogen sources on the production of RED compounds. Whole yeast was replaced with equal amounts of malt extract, soy, or

casein derived amino acids. Yeast extract was used in control cultures. Mycelia were collected by centrifugation for 10 minutes at 3040 x g in a swing-out bucket rotor in small scale production.

Russian yeast media was used in fermentations to produce large quantities of RED compounds. A 3L fermentation was inoculated with 50 mL of REDMBK6 preculture in Russian yeast media. The fermentation continued for 5 days at 30°C with stirring and aeration. *Streptomyces* cultures were checked for contamination with light microscopy. Cells were collected from 3L fermentations by centrifugation for 20 minutes at 7025 x g with a JA-10 rotor.

The strains predicted to produce polyenes were grown for 5 days at 30°C with vigorous shaking in 25 mL of Russian yeast media. The media contained either autoclaved baker's yeast or yeast extract to determine whether gene cluster expression was altered by the presence of whole yeast cells. Cultures were inoculated with 250 µl of mycelial cell preparations in 20% glycerol stored at -80°C.

3.3 Extraction of RED Compounds

The RED compounds were extracted from centrifuged cell pellets with a 1:1:1 methanol:toluene:0.1M phosphate buffer pH 7. Methanol was added first to lyse the cells and release the intracellular compounds. The methanol phase was then extracted with toluene, and the phosphate buffer was added to drive more of the hydrophobic RED compounds to the toluene phase. The toluene phase was subsequently extracted with phosphate buffer to remove cell membrane fats to the aqueous phase. The crude toluene extract was partially dried *in vacuo* at 77 bar and 40°C. The semi-dried extract was completely dried by nitrogen gas flow.

3.4 Extraction of Polyenes

Cell cultures were collected by centrifuging for 10 minutes at 3040 x g in a swing-out bucket rotor. The supernatant was discarded, and the cell pellets were extracted with 5 mL of methanol for 20 minutes at room temperature with gentle mixing. The samples were again centrifuged to separate cell debris from the crude extract. The supernatant was subsequently analyzed with analytical HPLC and LC-MS.

3.5 Silica Chromatography for RED Compounds

Dried RED compounds were re-solubilized in a minimal volume of 9:1 chloroform:methanol solution and applied to a normal-phase silica chromatography column. The silica was from Sigma-Aldrich. Sodium sulfate was used to remove trace amounts of water from the solvents before chromatography. Fractions were collected as they eluted from the column. The fractions were dried *in vacuo* and analyzed with analytical HPLC.

3.6 LH20 Chromatography for RED Compounds

An LH20 size-exclusion column, from Sigma-Aldrich, was prepared by suspending the resin in methanol and adding it to a glass column. The resin bed was equilibrated with a constant flow of 3 column volumes of methanol. Dried RED2 and RED3 extracts were solubilized in a minimal volume of methanol and applied to the column. Fractions were collected as the compounds eluted and were analyzed with analytical HPLC.

3.7 Analytical C18 HPLC

RED compound extracts were solubilized in HPLC grade methanol for analytical HPLC. Buffer A was aqueous with 15% MeOH and 0.1% formic acid, and Buffer B was MeOH

with 0.1% formic acid. The flow rate was 0.5 mL/min. The running method is shown in Table 1.

Crude methanol extracts from cells were screened for polyene production with analytical HPLC via the method shown in Table 2. Buffer A for the polyenes was aqueous with 15% acetonitrile and 0.1% formic acid, and Buffer B was acetonitrile. The flow rate was 0.5 mL/min.

For all compounds, the HPLC instrument was a Shimadzu model SCL-10AVP, and the column was a Kinetex reverse-phase 2.6u C18 100Å; 100 x 4.6 mm from Phenomenex (537743-29).

Table 1: Method for all HPLC and LC-MS runs in work with REDMBK6.

Time (min)	0	2	10	17	17.1	19	19.1	24
Buffer B	45%	45%	100%	100%	0%	0%	45%	45%

Table 2: Method for all HPLC and LC-MS runs for discovery of polyenes.

Time (min)	0	2	20	20.01	24	24.01	29
Buffer B	0%	0%	60%	100%	100%	0%	0%

3.8 Preparative C18 HPLC

Preparative HPLC was only run for the RED compounds. Dried silica chromatography fractions were re-solubilized in a minimal volume of 1:1 HPLC grade methanol and Mili-Q water. A 2 mL inoculation loop was filled with mili-Q water before a 1 mL injection of compound. Buffer A was aqueous with 15% MeOH and 0.1% formic acid, and Buffer B was 100% MeOH. The flow rate was 5.0 mL/min; the running method is shown in Table 1. The instrument was a Shimadzu model CBM-20A, and the column was a Sunfire: prep C18 5 µm 10 x 250 mm (column serial 163136081115 03).

3.9 LC-MS

The running conditions for the RED compounds on LC-MS were identical to those used for analytical HPLC; the method is shown in Table 1. The running conditions for analysis of crude polyene extracts with LC-MS were the same as those used for analytical HPLC, and the method is shown in Table 2. All compounds were solubilized in methanol for analysis. The column used for all samples was a Kinetex 2.6u C18 100A 100 x 4.6 mm from Phenomenex (537743-29), and the instrument was an Agilent 1200 HPLC with a Diode Array Detector. The compounds were ionized with electrospray ionization.

3.10 High Resolution MS for RED Compounds

Purified RED compounds were solubilized in methanol to determine exact masses with a Bruker Daltonics micrQTOF mass analyzer. The compounds were ionized with electrospray ionization and were analyzed in positive mode.

3.11 NMR for RED Compounds

Purified samples of RED2 and RED3 were prepared for NMR in deuterated methanol or deuterated chloroform, respectively. ^{1}H NMR and ^{13}C NMR 1D measurements, and COSY, HSQC-DE and HMBC 2D measurements were performed. The instruments used were a TYBruker600cryo with an actively shielded Bruker 600 MHz magnet, and an AABruker500cryo with an actively shielded Bruker 500 MHz magnet.

3.12 Antibiotic Activity Assay

Crude RED compounds or crude polyenes were solubilized in a minimal volume of chloroform and added drop-wise to a piece of filter paper. Excess chloroform was

evaporated in vacuo. Plain filter paper and filter paper soaked in chloroform were used as controls. Yeast was plated on a YPD plate (10 g/L yeast extract, 20 g/L peptone, 20 g/L glucose, 15 g/L agar) and the compound-loaded paper was placed in the center of the plate. The yeast was allowed to grow at 30°C for 24 hrs, and a zone of inhibition was observed.

3.13 Genomic DNA isolation

REDMBK6 was cultured for 3 days at 30°C with vigorous shaking in 25 mL GYM media (4 g/L glucose, 4 g/L yeast extract, 10 g/L malt extract, 1L mili-Q water) to produce cells for DNA isolation. Cell culture was centrifuged for 10 minutes at 3040 x g in a swing-out bucket rotor to yield a pellet. Genomic DNA was isolated from the REDMBK6 cell pellet with the Salting Out procedure from Pospiech, A. and Neumann, B. (1995) and sent for sequencing.

3.14 Spectrophotometry of RED2 at Varying pH Values

The absorbance maxima of RED2 was determined by solubilizing samples purified with preparative HPLC in 0.1M phosphate buffers of varying pH. The pH values of the phosphate buffers were adjusted by gradually adding 1 molar HCl and 1 molar NaOH until the desired pH values were achieved. The phosphate buffers ranged from pH 3 to pH 9. A few drops of RED2 solubilized in MeOH was added to each buffer in a cuvette, and the uv/vis absorbance spectra was measured with a Thermo Scientific Multiskan Go spectrophotometer.

4 Results:

4.1 Investigation of REDMBK6

4.1.1 Production of RED Compounds

The *Streptomyces* REDMBK6 was one of multiple strains isolated in a laboratory course. It was selected for further investigation because it produces RED2 and RED3 in transfer media only when whole yeast is used as a nitrogen source (Figure 13). The compounds are named based on when they elute from HPLC. These compounds were hypothesized to be polyene macrolide antibiotics, since production appeared to be dependent on the interaction between *Streptomyces* and intact yeast cells, and crude extracts had antifungal activity.

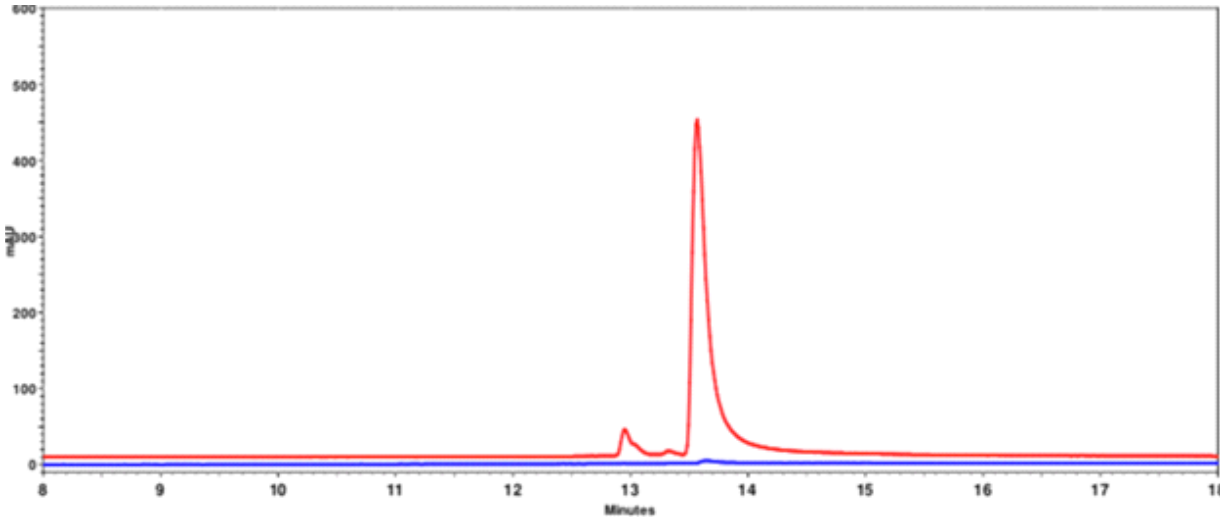

Figure 13: REDMBK6 production profiles in transfer media when whole yeast (red) and yeast extract (blue) are used as nitrogen sources. The chromatograms are shown at 530 nm. RED3 was primarily produced in the cultivation grown with whole yeast.

However, when media other than transfer media are used, REDMBK6 produces the compounds after 3 to 5 days of growth when cell density increases. Although the provided nitrogen source affects the ratio in which the compounds are produced, whole yeast cells are not necessary to elicit production in other media (Figure 14). REDMBK6 never achieves high cell density when grown in transfer media, and cell growth is only

discernible as the media becomes cloudy. The compounds are not produced in transfer media without the additional cell density attributed by whole yeast in culture.

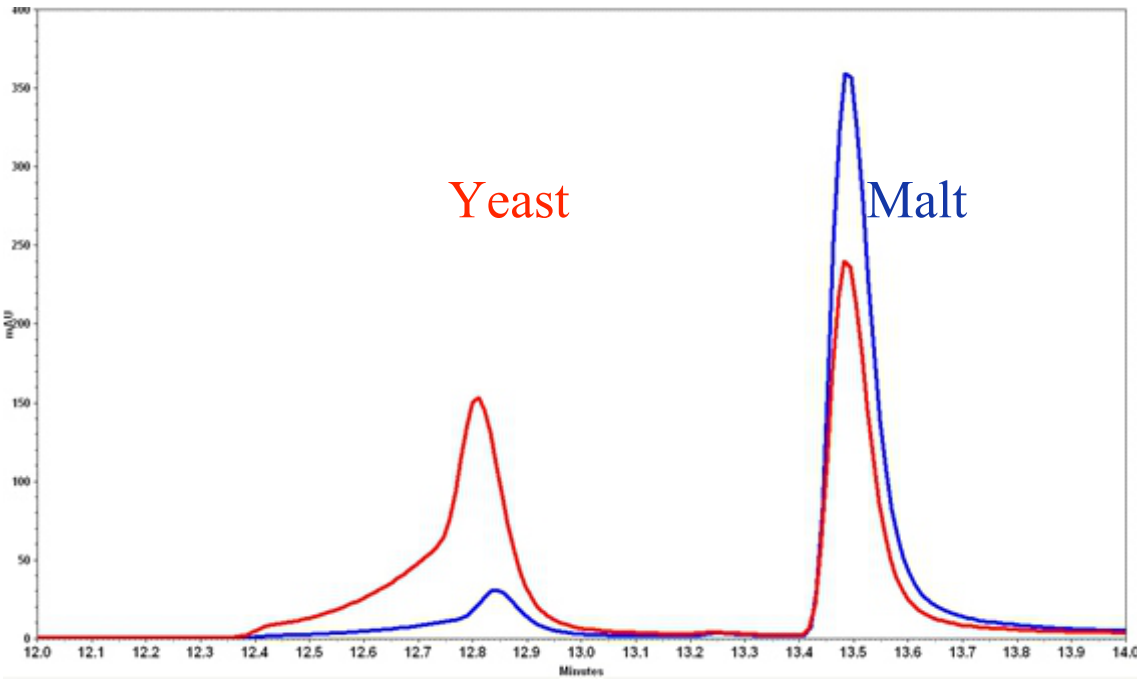

Figure 14: REDMBK6 production profiles in Russian yeast media when either whole yeast (red) or malt extract (blue) is used as a nitrogen source. Whole yeast causes RED2 and RED3 to be produced in similar amounts, and malt extract elicits production of primarily RED3. The chromatograms are shown at 530 nm.

RED2 and RED3 are produced in Russian yeast media after 3 to 5 days of growth, regardless of whether whole yeast is included in the culture. REDMBK6 cultures in Russian yeast media are dense with visible cell clusters in the media and cells collecting on the glass after 3 to 5 days. Compound production appears to be related to increased cell density. The compounds are produced in different ratios depending on the nitrogen source that is provided in Russian yeast media. Both compounds are produced in similar quantities when whole yeast is used, while malt extract elicits production of primarily RED3 (Figure 14). The compounds remain in the cells until they are extracted, and cell clumps turn red as culture density increases.

4.1.2 Spectral Properties of the RED Compounds

Extracts of RED2 and RED3 are red in neutral and acidic pH solutions and turn yellow in basic solutions. The absorbance maxima of purified RED2 were determined at varying pH values (Figure 15). Nitrogen was predicted to be present in the structure, since the color change is most dramatic between pH 5 and pH 6. Protonation and de-protonation of nitrogen atoms that are part of a conjugated system cause color change. The compounds have similar absorbance maxima near 530 nm in acidic solutions (Figure 16). The absorbance maximum of RED2 is a slightly shorter wavelength than that of RED3 in acidic solutions.

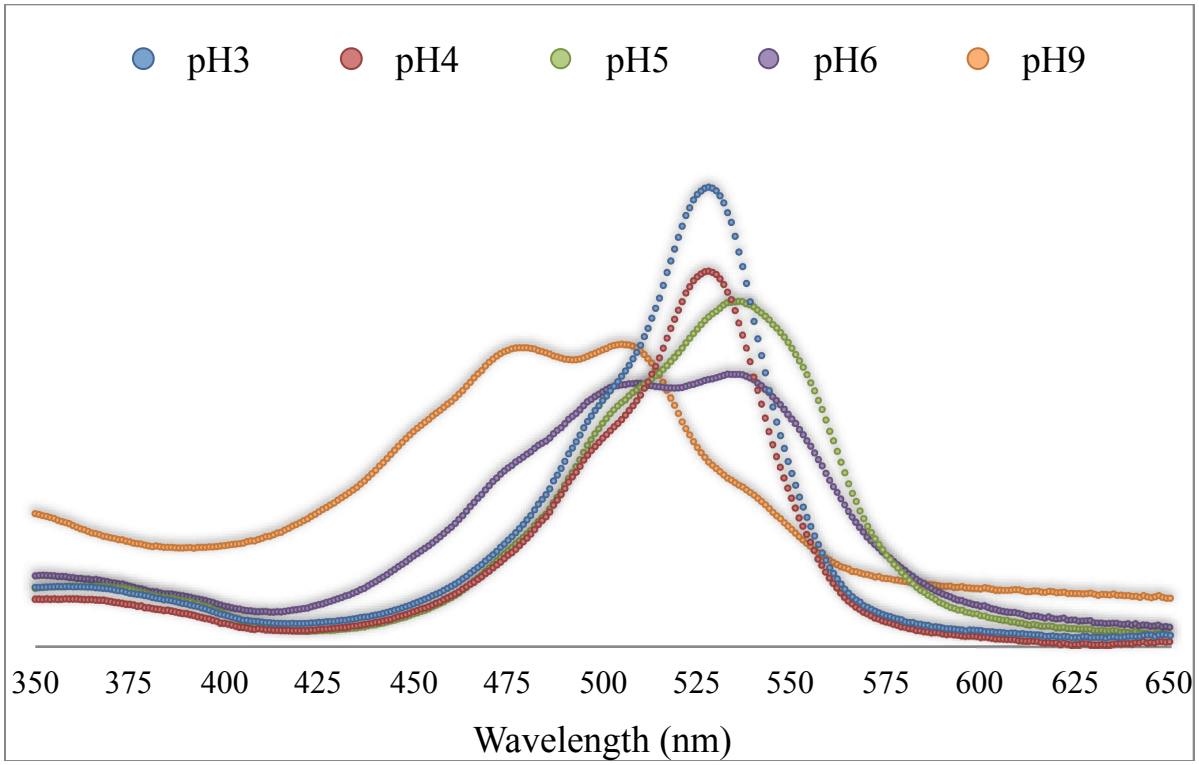

Figure 15: The absorbance maxima of pure RED2 undergoes a hypsochromatic shift as the pH increases to basic conditions. The most dramatic color change is observed between pH 5 and pH 6. The color change is attributed to the influence of pH on the nitrogen atoms which are part of the conjugated system of RED2.

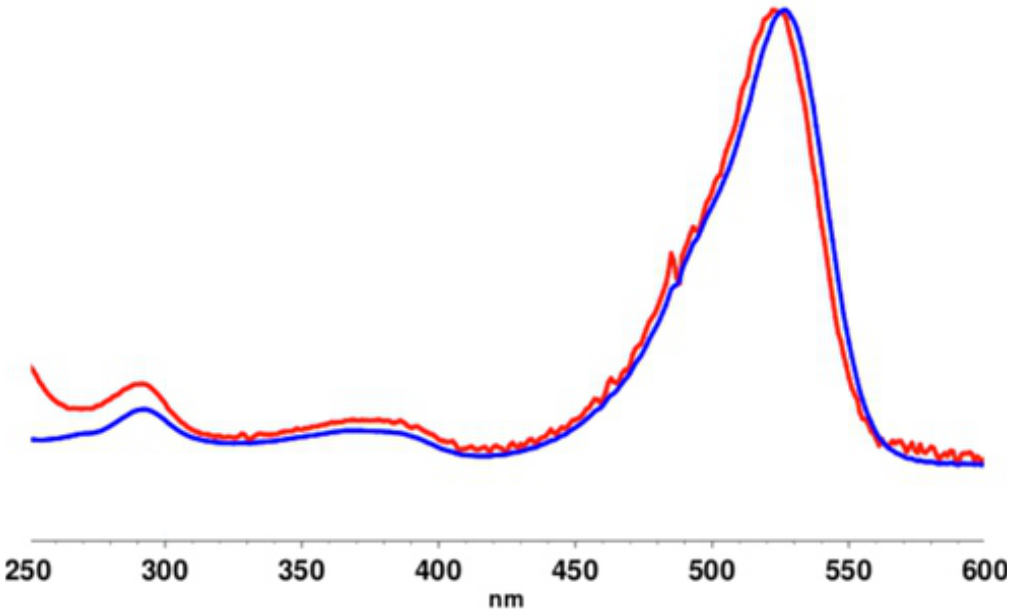

Figure 16: Absorbance maxima of RED2 (red) and RED3 (blue) in acidic conditions. The absorbance maximum of RED2 is a slightly shorter wavelength than RED3. The spectra were produced from a crude extract of the compounds analyzed with analytical HPLC in acidic conditions.

4.1.3 Antifungal Activity of RED2 and RED3

Figure 17: Zone of inhibition in an S. cerevisiae culture created by a crude extract of RED2 and RED3 after 24hrs incubation at 30°C. The filter paper was loaded with compounds solubilized in chloroform, then dried and applied to the plate at the time of inoculation. A control using filter paper soaked in pure chloroform had no activity.

Crude extract from a culture of REDMBK6 grown in Russian yeast media with whole yeast was solubilized in chloroform and loaded drop-wise onto a piece of filter paper. The dried filter paper was placed on a freshly inoculated YPD plate of *S. cerevisiae.* A zone of inhibition was observed after a 24 hour incubation at 30°C (Figure 17). A negative control was carried out using filter paper that was soaked in pure chloroform and then dried. A zone of inhibition did not result in the negative control, indicating that the antifungal activity resulted from the crude RED compound extract.

4.1.4 Structure Elucidation of RED2 and RED3 with NMR

RED2 and RED3 were purified using multiple two-phase organic extractions and chromatography techniques to produce samples suitable for analysis with NMR. RED2 was identified as metacycloprodigiosin, and RED3 was identified as undecylprodigiosin. The published structures are included as a reference (Figure 18) (Liu et al., 2005).

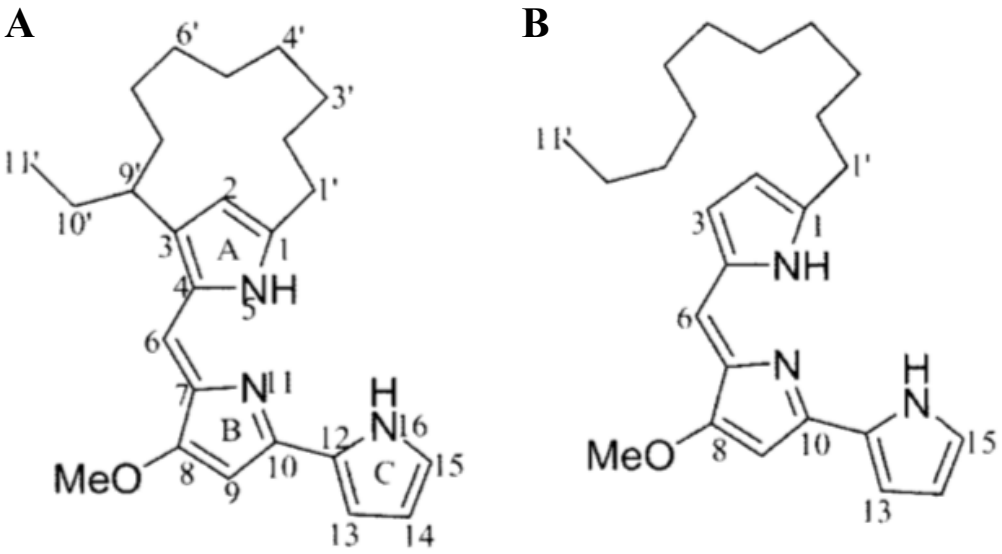

Figure 18: Published structures of metacycloprodigiosin or RED2 (A) and undecylprodigiosin or RED3 (B) (Liu et al., 2005).

The one dimensional (1D) ^{1}H NMR spectra of RED2 and RED3 show that the compounds have many aliphatic hydrogens with overlapping signals. The aliphatic region accounts for 22 hydrogen atoms in RED2 and 23 hydrogen atoms in RED3

(Figure 19). The coupling constants for the aliphatic hydrogens in RED2 could not be reliably discerned from the overlapping multiplets. The proximity of the signals is due to the hydrogens being in a similar chemical environment in the aliphatic ring structure (Figure 18A).

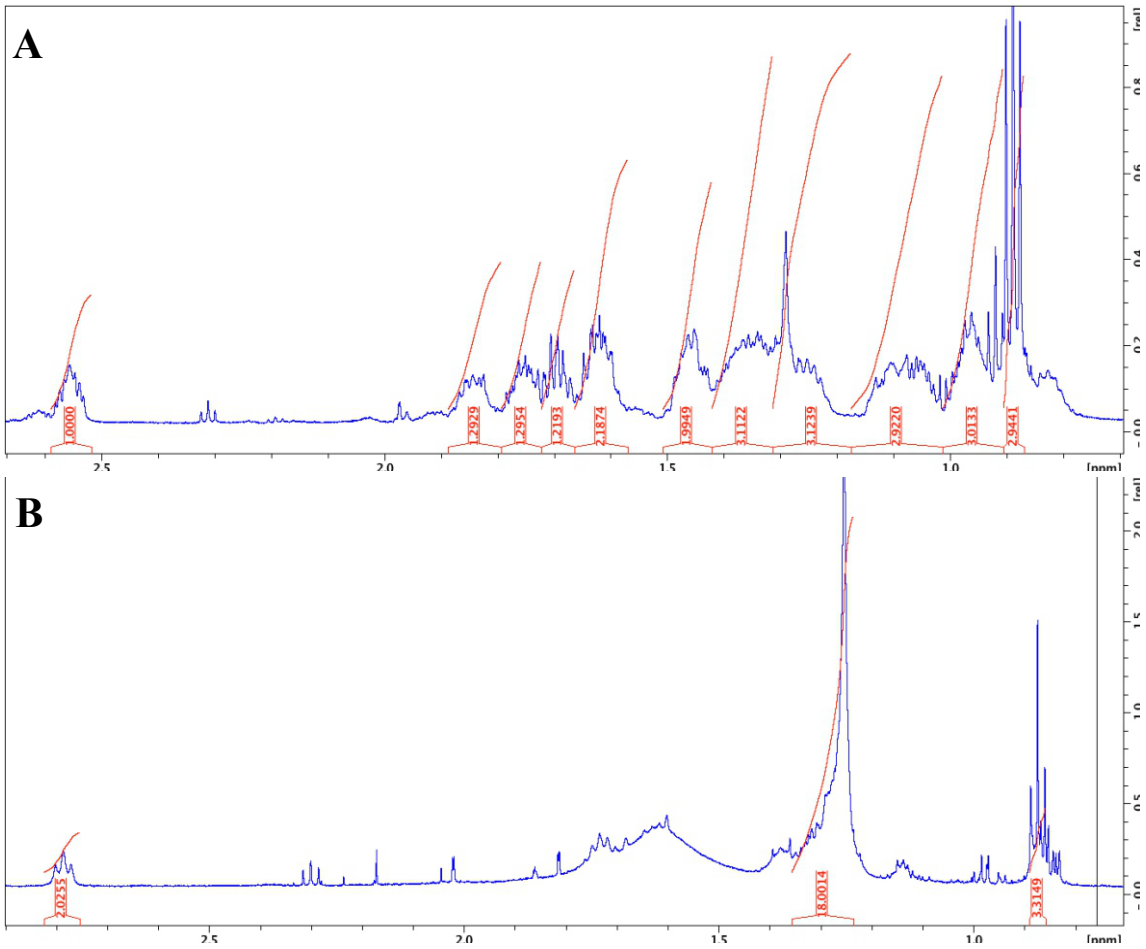

Figure 19: Aliphatic region of the ^{1}H NMR spectrum RED2 (A) in deuterated methanol and RED3 (B) in deuterated chloroform. The integrals indicate RED2 has 22 aliphatic hydrogens while RED3 has 23 aliphatic hydrogens. Integration was important for determining the number of hydrogen atoms represented by the overlapping multiplets.

The large peak in the RED3 proton spectrum represents the 18 hydrogen atoms on the open chain of nine CH_2 carbon atoms (Figure 19B). The hydrogens in the chain have nearly identical chemical shifts due to the free rotation around the carbon—carbon sigma bonds. The signal at 1.6 ppm is from water in the RED3 sample. The spectrum of

each compound has a triplet at 0.88 ppm with an integral of 3. This signal represents the 3 hydrogens at the end of the aliphatic carbon chain in each compound (Figure 18B).

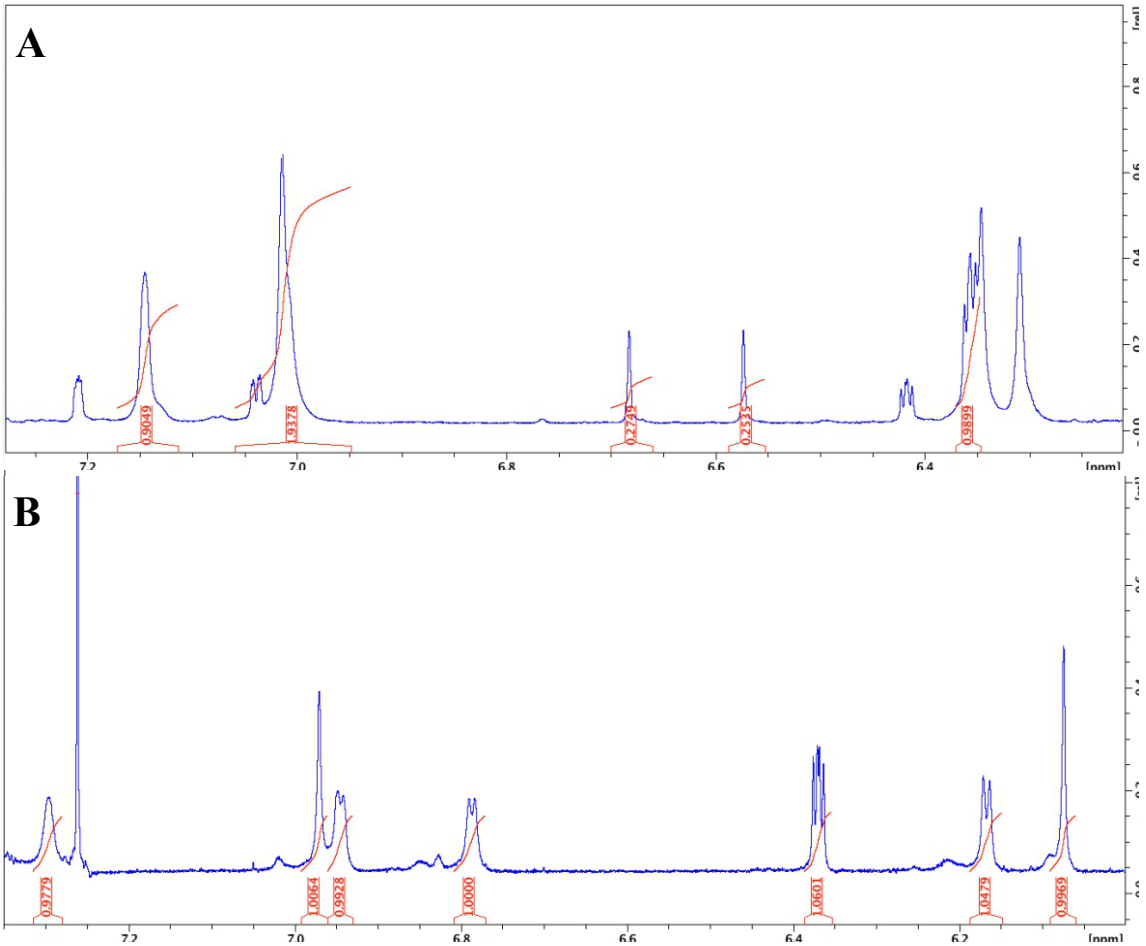

Figure 20: Aromatic region of the ^{1}H NMR spectrum of RED2 (A) in deuterated methanol and RED3 (B) in deuterated chloroform. The integrals indicate 6 aromatic hydrogens for RED2 and 7 for RED3. The signal in A at 7.1 ppm represents two hydrogens with overlapping signals. The largest singlet in B at 7.25 ppm is caused by chloroform.

The signals in the aromatic regions for each compound are fewer and less intense than the aliphatic signals (Figure 20). Hydrogen atoms on the rigid aromatic rings are further apart and in different chemical environments due to the rigidity of the aromatic rings. The aromatic signals are primarily singlets, since neighboring carbon atoms do not have hydrogen atoms bound. Two of the hydrogen signals in the aromatic region for RED2 have integrals that are less than 1 (Figure 20A). The chemical environment of the

hydrogen atoms may be unfavorable for NMR. These signals are still considered to be part of the molecule because they have strong correlations with well defined parts of the molecule in the 2D NMR measurements. All of the aromatic hydrogen signals in RED3 have integrals near 1 (Figure 20 B).

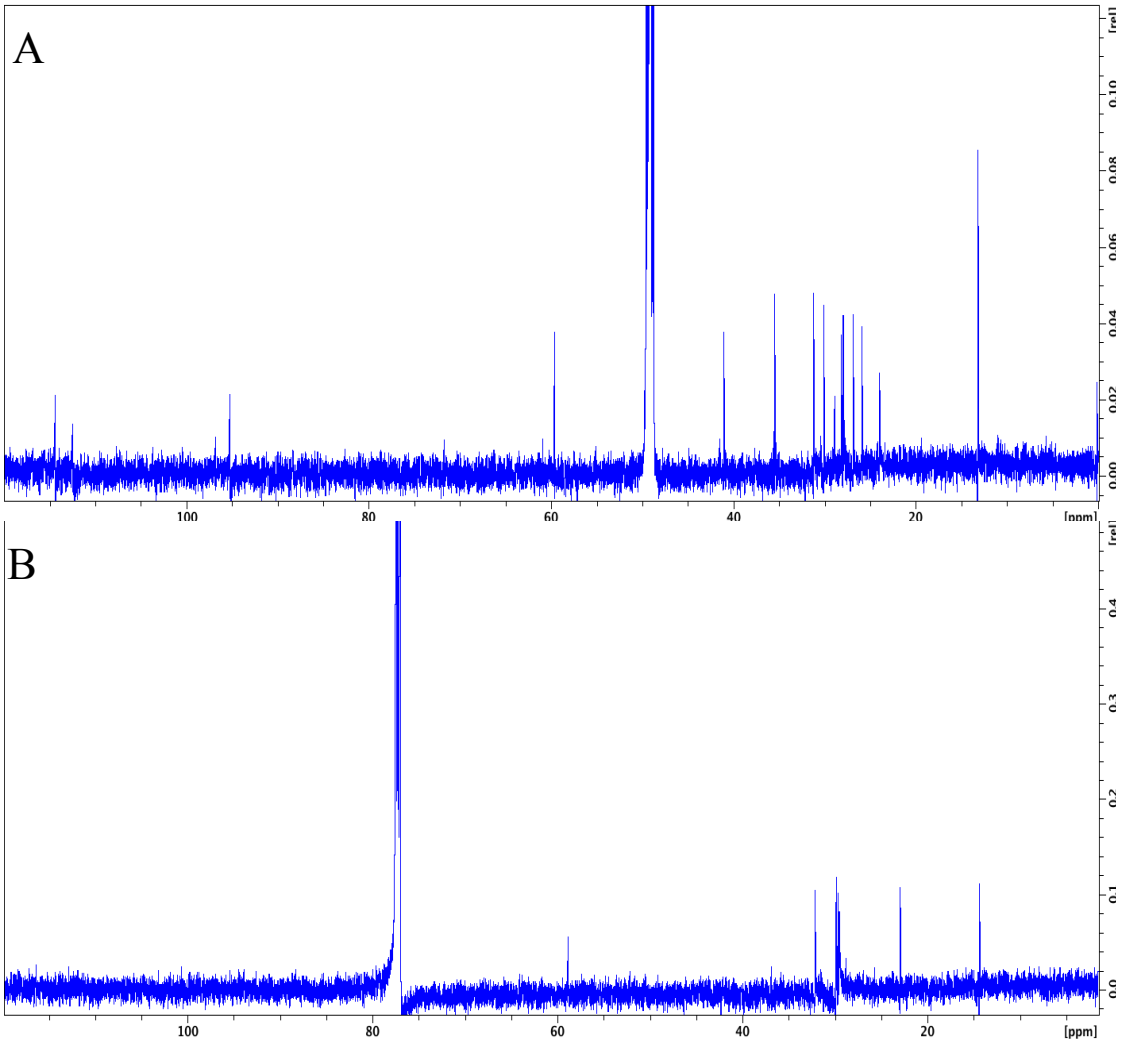

Figure 21: C13 NMR for RED2 (A) in deuterated methanol and RED3 (B) in deuterated chloroform. The largest peak in each spectra is from the solvent. Primarily aliphatic carbon atoms bound to hydrogen are visible in C13 NMR. Fully substituted and aromatic carbons give weaker signals.

The C13 carbon spectra for the compounds give an indication of how many carbon atoms are in each compound (Figure 21). Differences between the spectra are due to the use of deuterated methanol for RED2 and deuterated chloroform for RED3. Both

compounds have 28 carbons, although many quaternary carbon signals are too weak to be visible above the noise in the 1D measurements.

Two dimensional (2D) spectra are used to determine the intramolecular interactions between all hydrogen and carbon atoms. Fully substituted and aromatic carbon atoms with weak signals that were indiscernible from background noise in the C13 measurements were inferred by using HSQC-de and HMBC. Weak carbon signals that correlated with at least two hydrogens, which had integrals of at least 1, were considered to be legitimate carbon signals. HSQC-de shows which hydrogens are bound to which carbons and the hybridization state of the carbons (Figure 22). Blue signals in HSQC-de indicate a CH_2 while green signals indicate either a CH or a CH_3.

The HSQC-de for the aliphatic region of RED2 shows many pairs of hydrogen atoms, which have different chemical shifts, bound to the same CH_2 carbon. This phenomenon occurs in aliphatic rings because the two hydrogen atoms are held on different planes of the ring and interact differently with the magnetic field during NMR acquisition. The HSQC-de for RED3 has fewer signals because the aliphatic region has an open chain conformation where the atoms can rotate freely around the carbon—carbon sigma bonds.

COSY 2D spectra show the interactions between the hydrogen atoms on neighboring carbon atoms (Figure 23). Unconnected fragments of the structure of RED2 were inferred by recognizing which hydrogen atoms interacted, and referencing HSQC-de to find the partnered carbon atoms. 1D hydrogen spectra are used as the reference in COSY spectra. The peaks in the diagonal line in every COSY spectrum results from the signal each hydrogen has for itself. A COSY signal indicating hydrogens on adjacent carbons was only considered valid if the signal was mirrored across the diagonal line.

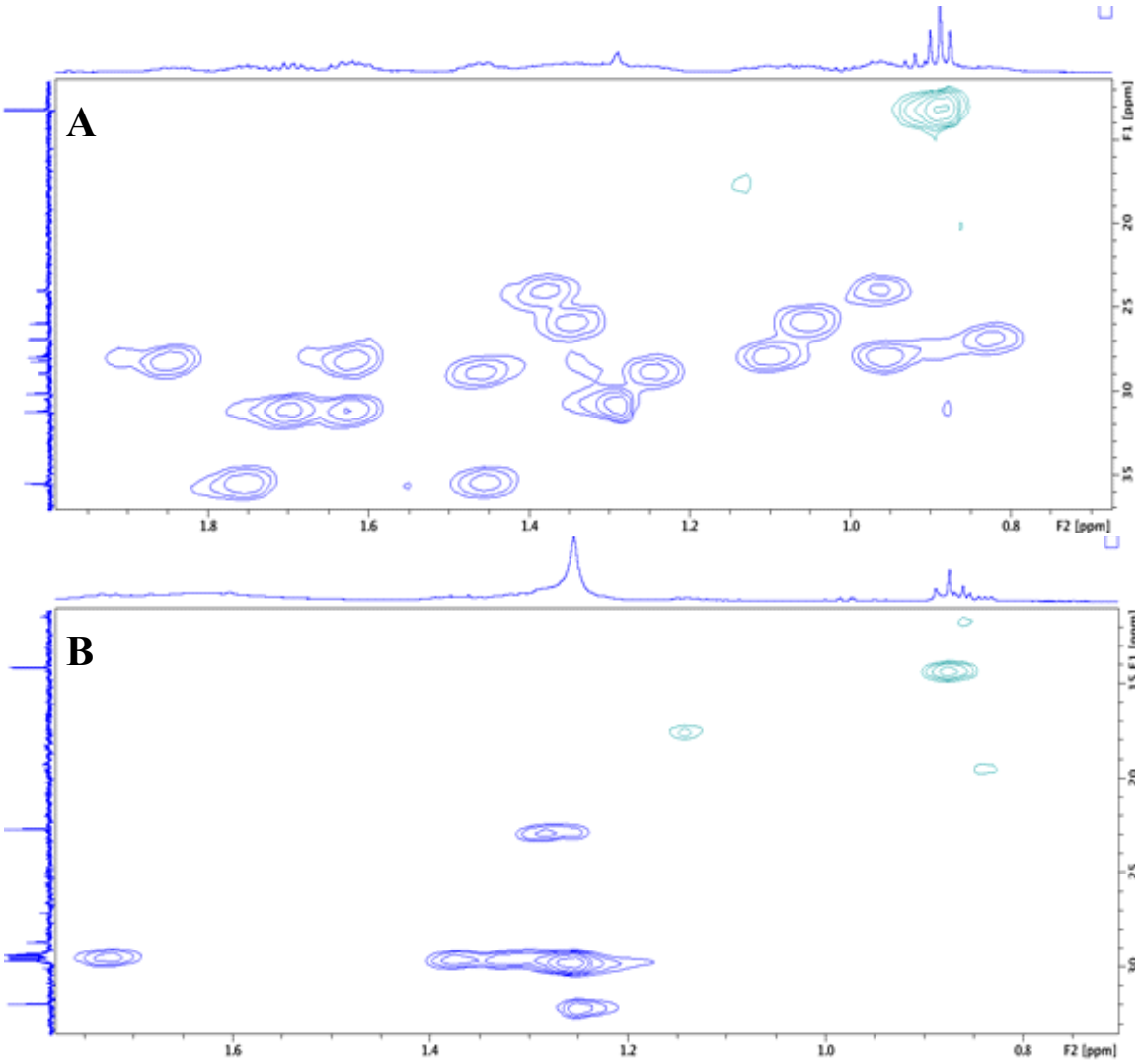

Figure 22: HSQC-de 2D spectra for the aliphatic regions of RED2 (A) and RED3 (B). The x-axis shows hydrogen shift, the y-axis shows carbon shift. Blue signals represent CH_2 groups and the green signals represents CH_3 groups. Blue signals on the same Y-plane indicate hydrogen atoms bound to the same carbon atom. HSQC-de is valuable for identifying carbons which have signals indiscernible from background noise.

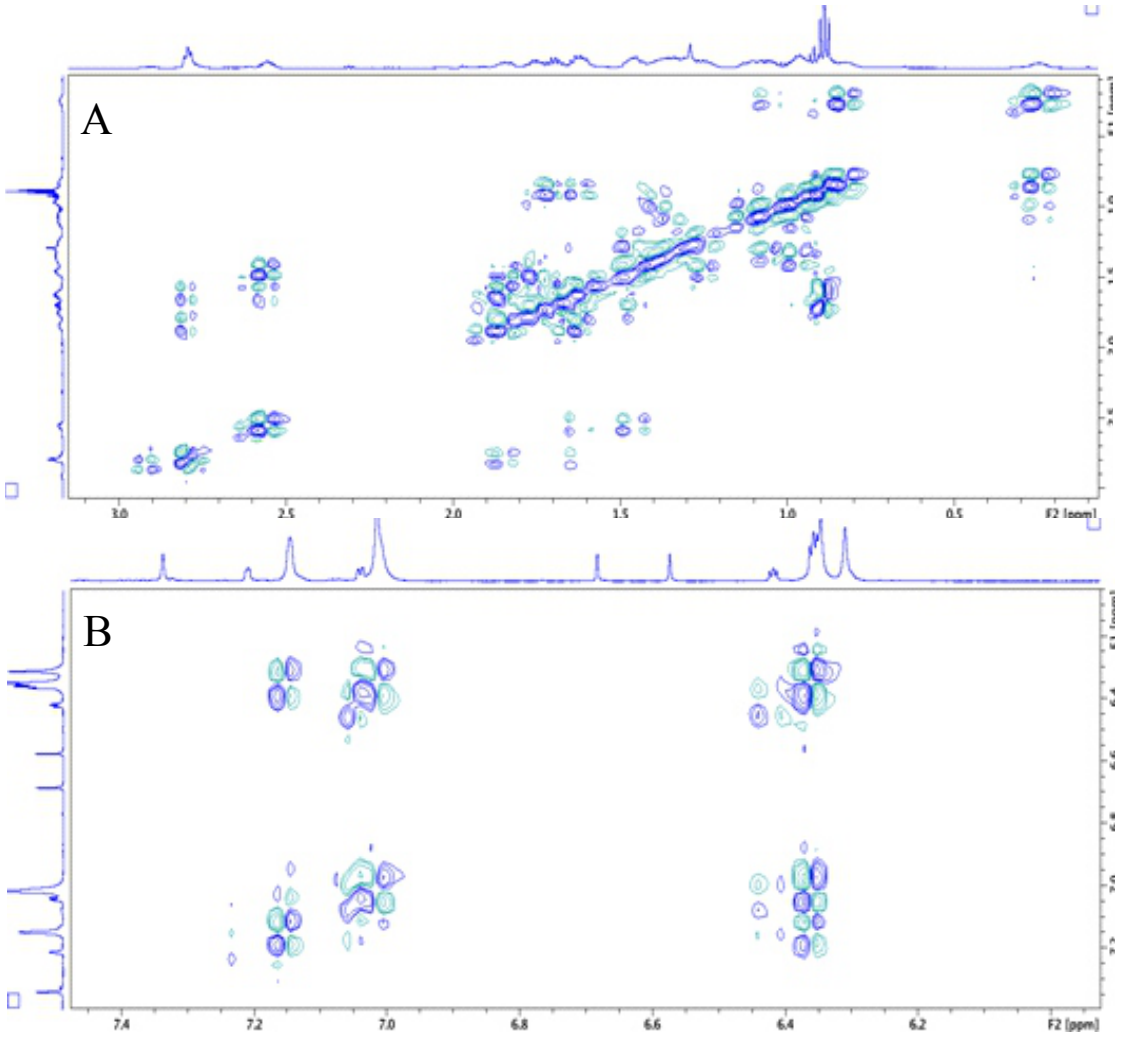

Figure 23: COSY data for RED2 aliphatic (A) and aromatic (B) regions. Signals indicate relationships between hydrogen atoms on adjacent carbons. COSY is most valuable when the coupling constants for hydrogen signals are overlapping or singlets.

HMBC signals represent interactions between a reference hydrogen and multiple distal carbons atoms (Figure 24). The distance of the carbons from the reference hydrogen varies depending on the structure of the molecule. In this study, carbons were at most three sigma bonds away from the reference hydrogen atom. HMBC was used to piece together the fragments of the molecules that become apparent with the COSY spectra. COSY measurements were crucial, since coupling constants could not be reliably determined for the crowded hydrogen signals in the aliphatic region (Figure 19). The fragments of the RED2 structure inferred with COSY were partially assembled using

HMBC data (Figure 25). Chemical shifts for the carbons and their associated hydrogens are given for RED2 in Table 3.

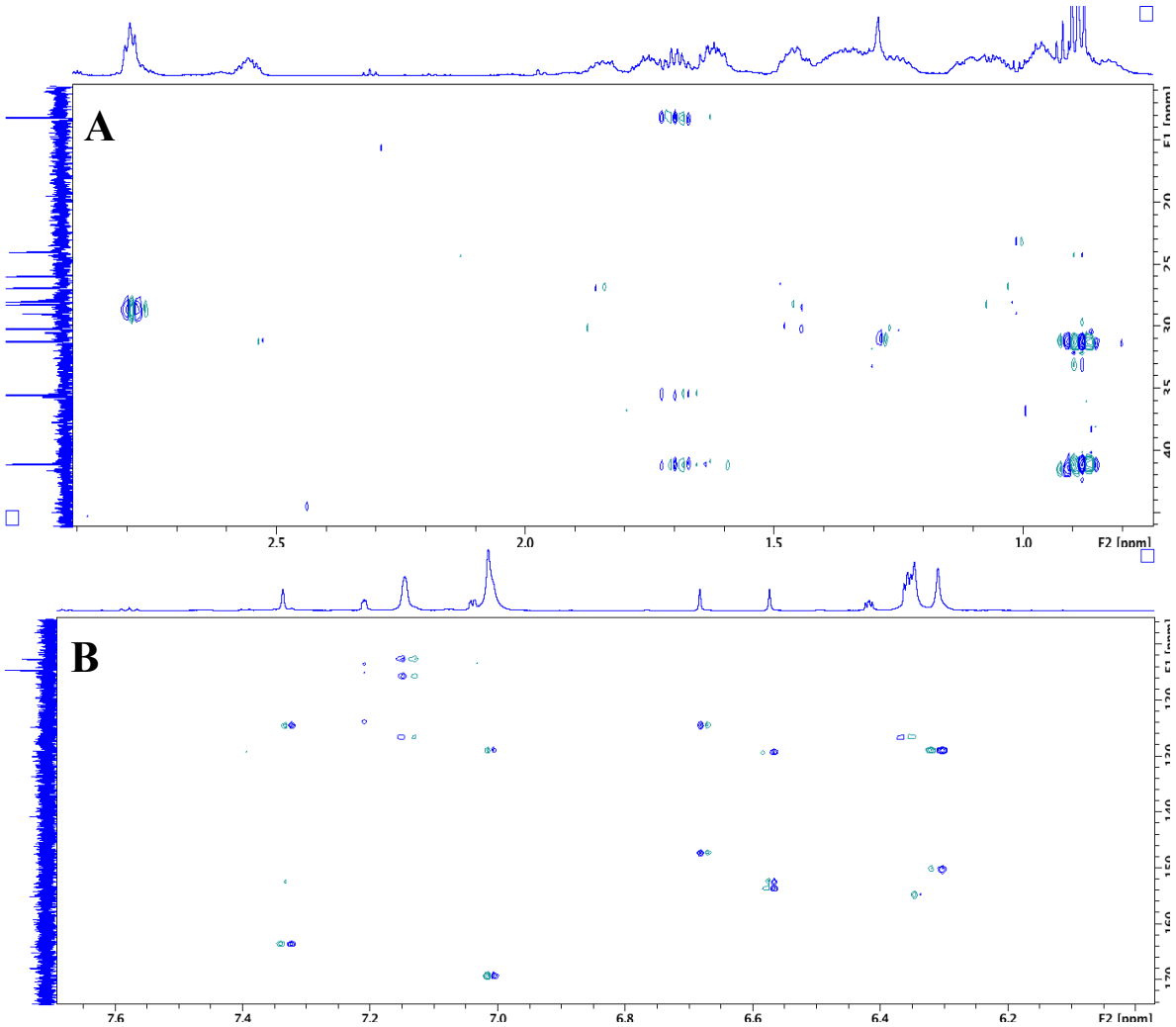

Figure 24: HMBC for the aliphatic (A) and aromatic (B) regions of RED2. Hydrogen spectra are on the x-axis and carbon spectra are on the y-axis. Signals indicate the interactions between hydrogens and distal carbons. Fully substituted carbon atoms with weak signals indiscernible from background noise are identified and verified as part of the structure with HMBC.

Table 3: ^{1}H- and ^{13}C-NMR data acquired for RED2 in deuterated methanol. Carbons in the rigid aliphatic ring have two hydrogens with different shifts. Numbering of carbons, as in Figure 25, is non-sequential due to nitrogens present in the structure.

Carbon Number	Carbon Shift (ppm)	Hydrogen Shift (ppm)
1	153.6	n/a
2	114.88	6.57
3	152.44	n/a
4	128.86	n/a
6	114.374	7.01
7	154.9	n/a
8	169.2	n/a
9	95.221	6.33
10	124.6	n/a
12	126.4	n/a
13	125.8	7.14
14	112.5	6.35
15	115.54	7.04
1'	30.16	2.79; 2.9
2'	28.173	1.615; 1.845
3'	28.874	1.24; 1.46
4'	26.855	0.24; 0.82
5'	25.895	1.05; 1.34
6'	23.947	0.961; 1.38
7'	27.931	0.952; 1.09
8'	35.433	1.45; 1.75
8 Ome	59.604	4.03
9'	41.01	2.55
10'	31.162	1.624; 1.69
11'	13.131	0.88

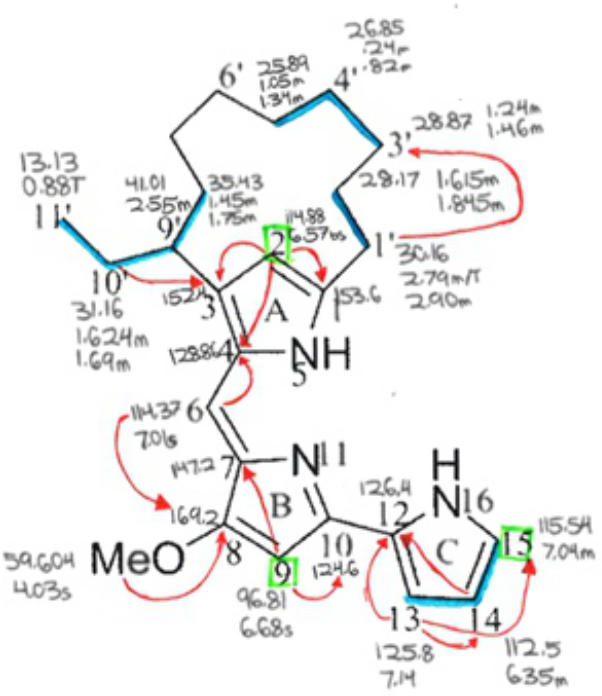

Figure 25: Structure of RED2 (metacycloprodigiosin) with NMR 2D spectral information drawn in. COSY relationships are in blue, and red arrows indicate HMBC. The green boxes indicate hydrogen atoms which had integrals smaller than 1. HMBC interactions were used to confirm that these hydrogen signals were genuine and were part of the structure. Only RED2 is shown since the NMR data for RED3 was analyzed by a colleague. Chemical shifts are written next to the corresponding carbons and hydrogens. This figure is altered from Liu et al., 2005.

4.1.5 Masses of RED2 and RED3

The exact masses were determined with high resolution MS in positive mode. RED3 has an exact mass of 393.2801 [394.2801 M+H]$^+$ and RED2 has an exact mass of 391.2585 [392.2585 M+H]$^+$. RED3 is two mass units heavier than RED2, indicating two additional hydrogens in RED3 (Figure 26). The compounds were ultimately identified as metacycloprodigiosin (RED2) and undecylprodigiosin (RED3) when genetic information for REDMBK6 became available (Figure 27). RED3 has two additional hydrogens because its aliphatic carbon chain is open, and the molecule has one less carbon—carbon sigma bond.

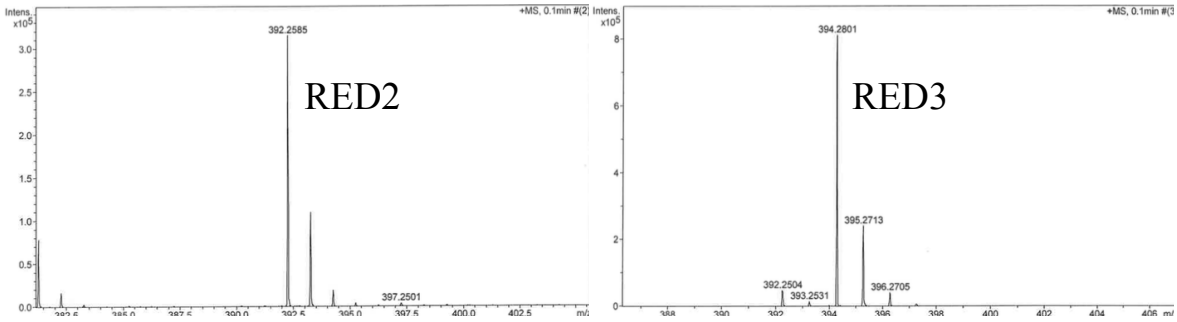

Figure 26: Exact masses of RED2 [392.2585 M+H]$^+$ and RED3 [394.2801 M+H]$^+$ were determined by high resolution MS in positive mode. RED2 has two fewer hydrogens due to the cyclized aliphatic carbon chain.

4.1.6 Biosynthetic Gene Cluster and Published Structures

Genome sequencing of REDMBK6 revealed a biosynthetic gene cluster that was predicted to produce metacycloprodigiosin and undecylprodigiosin. These compounds match the elucidated structures of RED2 and RED3, respectively. AntiSMASH revealed a BGC from REDMBK6 that has 90% gene similarity to a known prodigiosin producing cluster (Blin et al., 2017). NMR data from this study was fit to the published structures and the accompanying NMR data from Liu et al. (2005).

Figure 27: Gene cluster for undecylprodigiosin in Streptomyces REDMBK6. The SARP family regulator is indicated. Core biosynthetic genes are red, other biosynthesis genes are pink, regulatory genes are green, and other genes are grey. The core biosynthetic genes primarily encode polyketide synthase enzymes. The regulatory genes encode a SARP regulatory protein and a DNA binding response regulator.

4.2 Activation of Polyene Gene Clusters

4.2.1 Genome Mining

Genome mining of the in-house strain collection revealed three strains which have t1PKS clusters containing a cholesterol oxidase encoding gene (Figure 28). These clusters are typical of polyene macrolides, and showed sequence similarity to BGCs known to produce polyene macrolides. The relevant clusters were found in JCM 4712 and ATCC 27952 using the Artemis genome browser and AntiSMASH 4.1.0. The cholesterol oxidase gene within each cluster was identified by protein BLAST analysis (Camacho et al., 2009). Cholesterol oxidase was found in the BKMA 840 genome with Artemis, but the gene was not within a cluster identified by AntiSMASH 4.1.0. None of the clusters identified by AntiSMASH had more than 70% gene sequence similarity with a known compound. This degree of diversity is common amongst different polyene macrolide BGCs. (Carver et al., 2012; Blin et al., 2017)

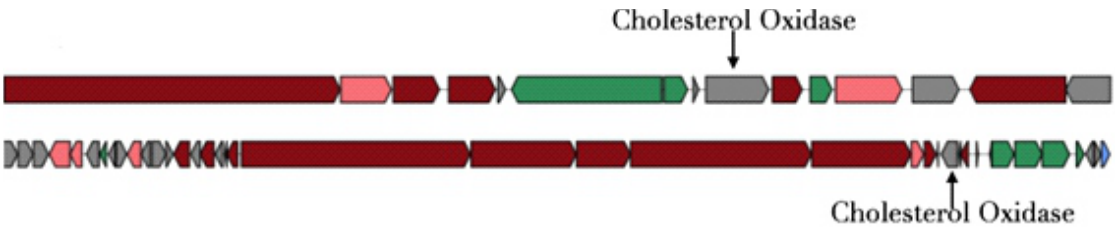

Figure 28: The t1PKS gene clusters from JCM 4712 (top) and ATCC 27952 (bottom) suspected to produce the polyenes. Core biosynthetic genes are red, other biosynthesis genes are pink, regulatory genes are green and other genes are grey.

4.2.2 Polyene Production

The strains *S. peucetius* ATCC 27952, *S. lavendulae* BKMA 840 and *S. hygroscopicus* JCM 4712 produce multiple compounds in large quantities only when cultivated with whole yeast. Minimal amounts of the main products are visible on analytical HPLC in crude methanol extracts from cultures grown with yeast extract (Figures 29–31). The

main product from each strains is produced in at least ten-times greater quantities in cultures containing whole yeast than in cultures containing yeast extract. Crude extracts from all of the strains that produced polyenes appeared slightly yellow. Cultures with greater *Streptomyces* biomass produced the most compounds. The wavelength in all of the presented chromatograms is 358nm. This wavelength is an absorbance maximum for all of the major products from the analyzed strains and indicates that the products are pentaenes. The minor peaks are likely compounds at different stages in the biosynthesis of the major compounds, since they have the same absorbance maxima.

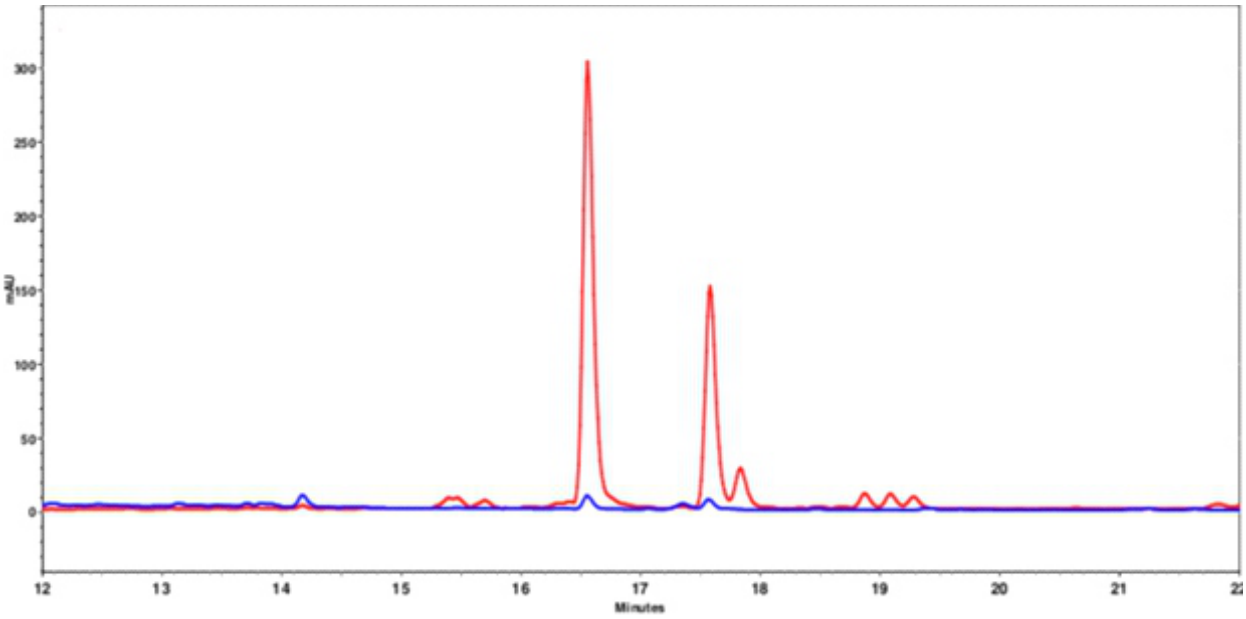

Figure 29: HPLC chromatograms of methanol extracts from ATCC 27952 at 358nm when grown with yeast (red) and without yeast (blue).

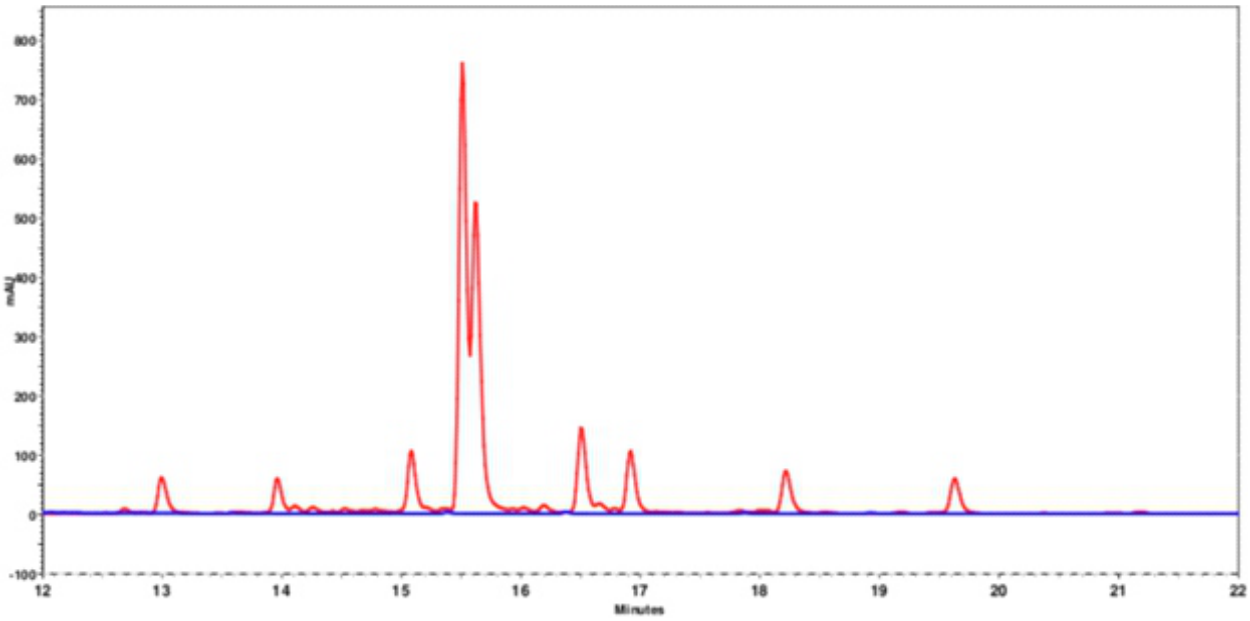

Figure 30: HPLC chromatograms of methanol extracts from BKMA 840 at 358nm when grown with yeast (red) and without yeast (blue). Major product peaks overlap.

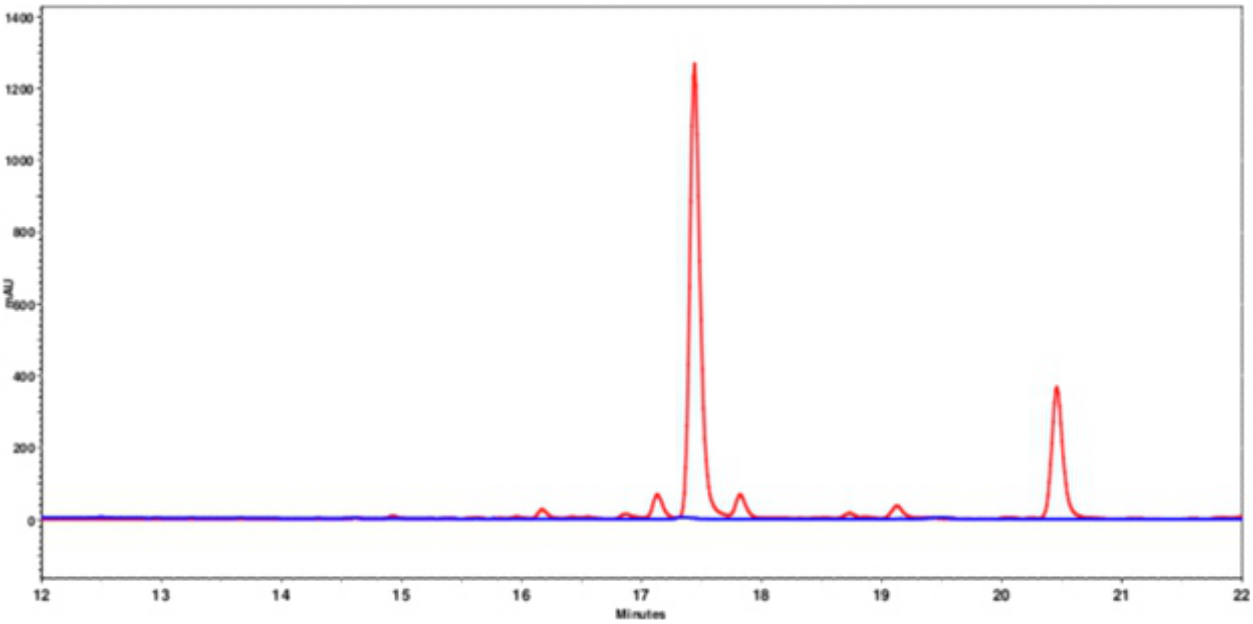

Figure 31: HPLC chromatograms of methanol extracts from JCM 4712 at 358nm when grown with yeast (red) and without yeast (blue).

4.2.3 Analysis of Produced Compounds

The major and minor compounds all have absorbance spectra maxima characteristic of polyene macrolides with three maxima peaks (Figure 32). The longest wavelength of the uv/vis absorbance maxima for all of the major products from co-cultures was 358 nm.

The other two uv/vis absorbance maxima for the major compounds are 338 nm and 322 nm. Pentaenes have three uv/vis absorbance maxima between 300 nm and 400 nm (Thomas, 1976). Crude methanol extracts from mycelia appear slightly yellow when polyenes are present.

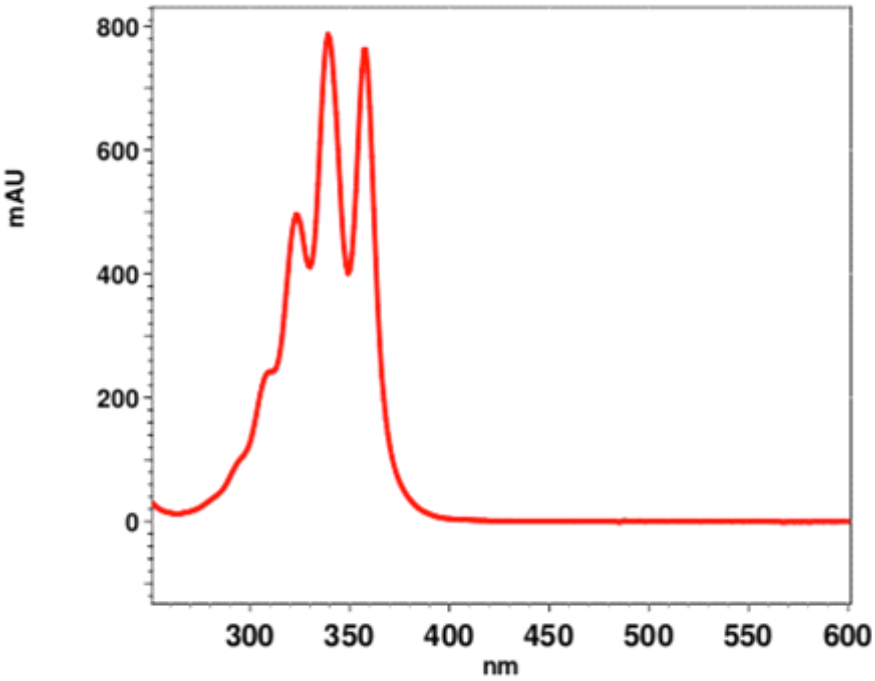

Figure 32: Absorbance spectrum of the main polyene product from BKMA 840 when grown in Russian yeast media containing whole yeast. Maxima are 358nm, 338nm and 322nm. All products from the selected strains had similar uv/vis spectra.

Crude extracts of the cultures grown with whole yeast have antifungal activity against *S. cerevisiae* grown on a YPD plate (Figure 33). After one day of growth at 30°C, a zone of inhibition, where yeast did not grow, was visible around the filter paper loaded with compound extract. Extracts from the whole yeast cultures were yellow when concentrated. The extract from the culture grown with yeast extract was clear, and no zone of inhibition was observed. Results from the negative control and the yeast extract culture were identical, indicating that the zone of inhibition was caused by the extracted compounds.

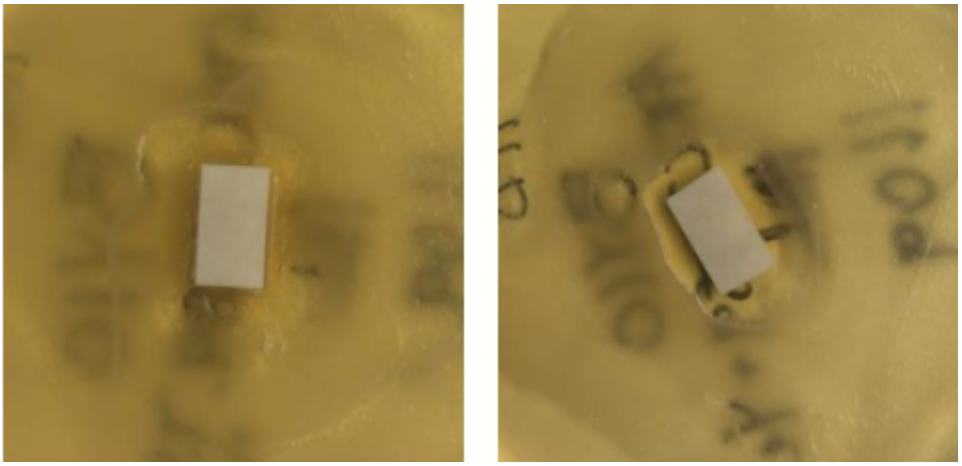

Figure 33: Antibiotic activity assay with crude methanol extract from JCM 4712 mycelia grown without yeast (left) and with yeast (right). A zone of inhibition is visible around the filter paper loaded with extract from the JCM 4712 culture grown with whole yeast.

4.2.4 Mass Spectrometry of Produced Compounds

Crude methanol extracts from the three strains which produce polyenes when grown with whole yeast were analyzed with low resolution LC-MS (Figures 33–36). The wavelength used for all of the chromatograms was 358nm. The compounds did not ionize in positive mode, and all of the extracted ion masses are reported in negative mode. The masses of the major products which have an absorbance maximum at 358 nm were between 535 amu and 667 amu. Small-sized polyenes typically fall within this mass range (Thomas, 1976). ATCC 27952 and BKMA 840 produced larger compounds in lesser amount with masses of 926 amu and 1021 amu, respectively.

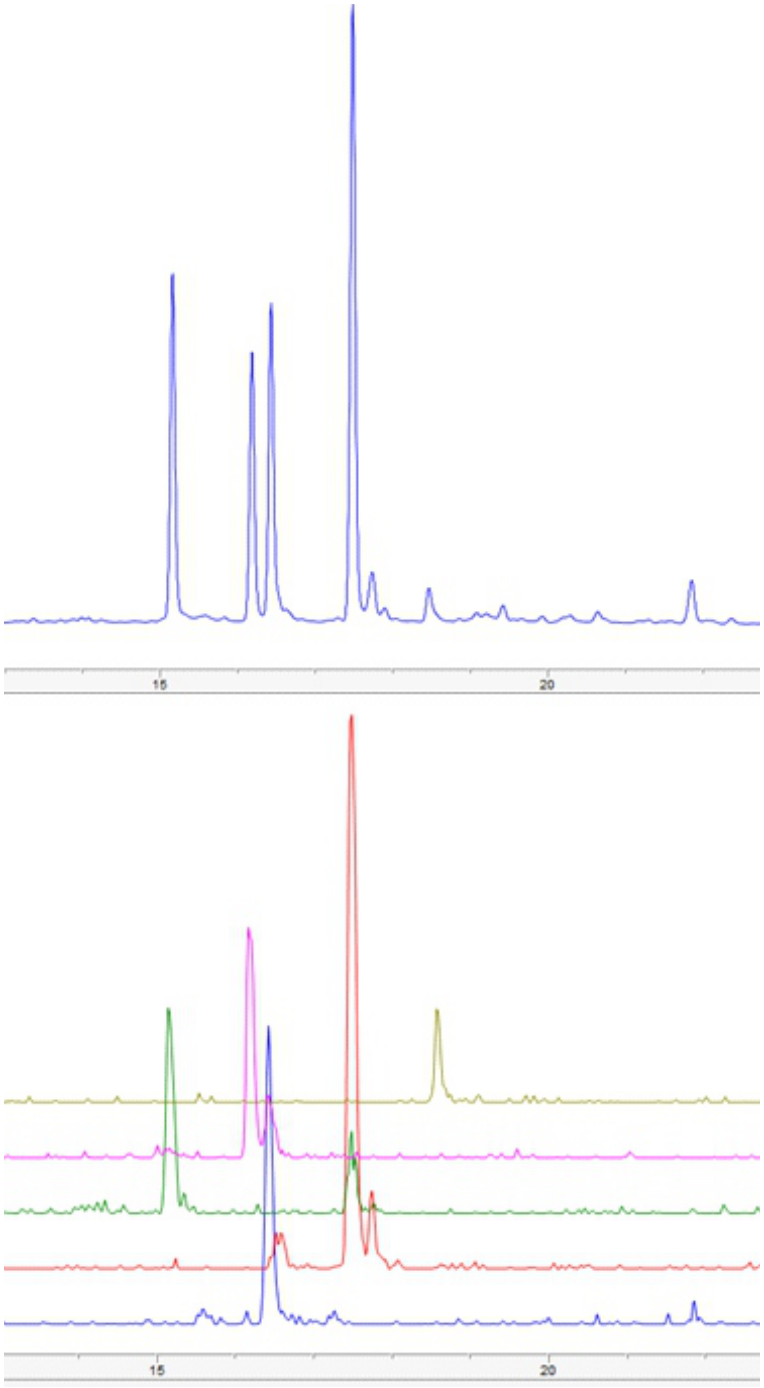

Figure 34: Absorbance shown at 358nm (top) and extracted ions (bottom) of the main products from ATCC 27952 cultured with yeast. The extracted ion masses in negative mode are 591 (blue), 605 (red), 607 (green), 621 (pink) and 925 (yellow).

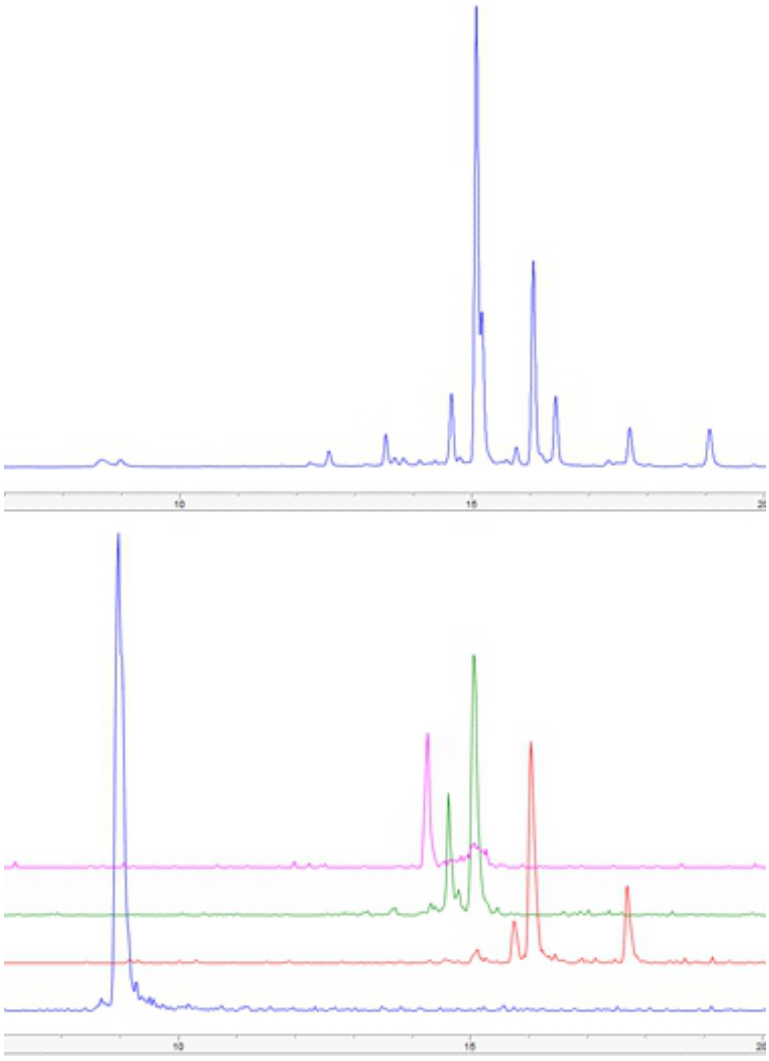

Figure 35: Absorbance shown at 358nm (top) and extracted ions (bottom) of the main products from BKMA 840 cultured with yeast. The extracted ion masses in negative mode are 603 (blue), 635 (red), 651 (green) and 1020 (pink).

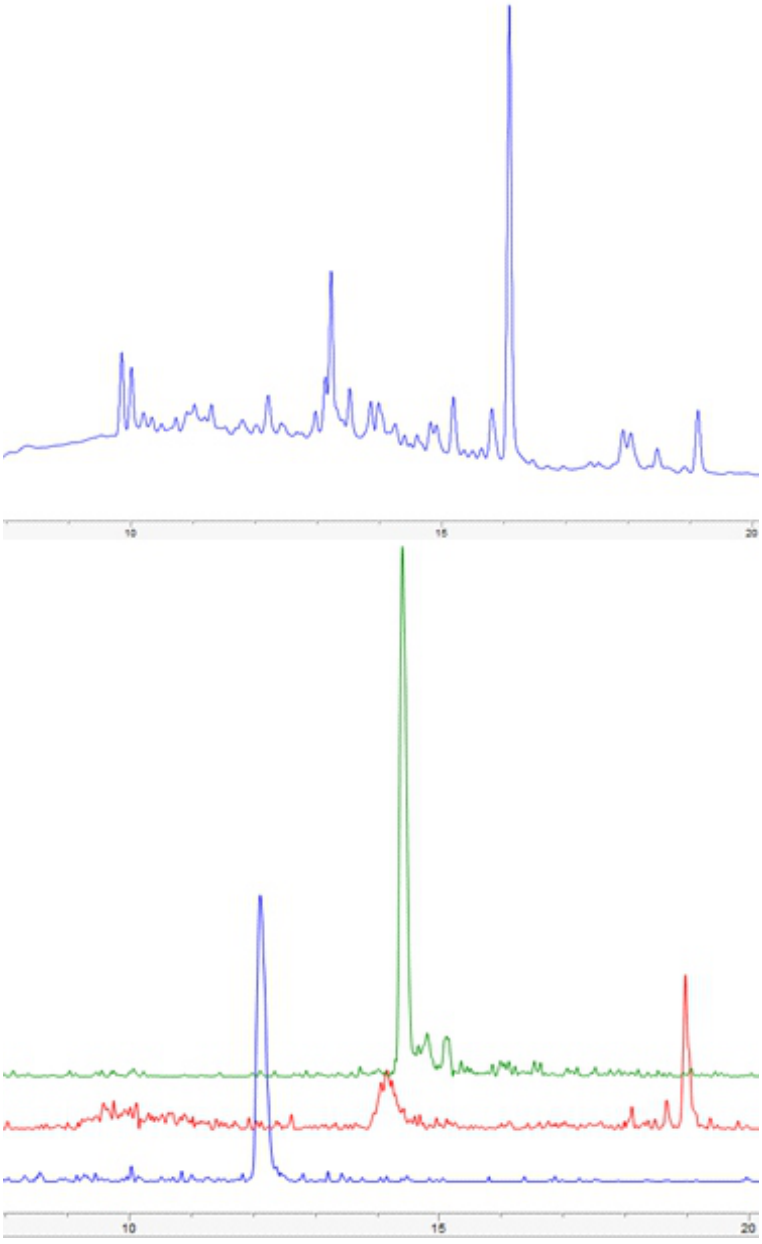

Figure 36: Absorbance shown at 358nm (top) and major products ionized in negative mode (bottom) from JCM 4712 cultured with yeast. The extracted ion masses in negative mode are 535 (blue), 635 (red) and 666 (green).

5 Discussion:

5.1 Streptomyces REDMBK6 and the RED Compounds

5.1.1 Identification of Metabolites from Streptomyces REDMBK6

The laboratory course isolate *Streptomyces* REDMBK6 was singled out for additional analysis because it was observed to produce red colored compounds with antifungal activity only when it was grown with whole yeast. The bioactive compounds were believed to be polyenes, since the production appeared to be elicited by an interaction of the *Streptomyces* with a fungi (Mendes et al., 2007). However, the yeast-dependent production of the RED compounds was observed when REDMBK6 was cultured in transfer media. REDMBK6 never achieves a high cell density in transfer media, and the strain was eventually shown to produce the red compounds in Russian yeast media, regardless of whether yeast was included in the media. The implication of cell density on the regulation of the production of RED2 and RED3 is discussed in section 5.1.3.

NMR analysis and genomic information on REDMBK6 were used to identify RED2 and RED3 as metacycloprodigiosin and undecylprodigiosin, respectively. The fragments of the structures that had been solved using HSQC-de, COSY and HMBC were assembled via comparison to the published structures as a guide (Figure 25). (Liu et al., 2005)

Expectations that RED2 and RED3 were polyenes hampered structure elucidation. The HSQC-de signals from the aliphatic region of RED2 seemed to support the polyene macrolide hypothesis because they indicate a large ring structure (Figure 22A). In this region, each carbon has two hydrogen atoms which have different chemical shifts. The difference in hydrogen shifts is caused by how the hydrogen atoms held on opposite sides of the ring structure interact differently with the NMR magnetic field.

The proton spectrum of RED3 in Figure 19B has one main peak for 18 aliphatic hydrogens because the molecule has an open conformation, and the atoms can move freely around the sigma bonds. All of the interactions of these hydrogens with the magnetic field is on average equal, so equivalent chemical shifts result. The same is true for the carbon atoms in the aliphatic chain which all have chemical shifts of about 30 ppm (Figure 21B). The similarity of the shifts for the hydrogens and carbons in the chain is clear in Figure 22B.

5.1.2 Regulation of Undecylprodigiosin and Metacycloprodigiosin Production in Streptomyces REDMBK6

Undecylprodigiosin and metacycloprodigiosin are part of the prodigiosin family of compounds, and they have been described in multiple species of bacteria. Metacycloprodigiosin is one possible cyclized derivative. The role of these compounds in bacteria is not well understood, but general antimicrobial activity and UV protective properties benefit the producing microbe. Evidence suggests that undecylprodigiosin has anti-oxidative properties; producing cultures challenged with peroxides have better survivability. In addition, prodigiosins are antimalarial and immunosuppressive and have selective cytotoxic activity against breast cancer cells (Narva & Feitelson 1989; Stankovic et al., 2012). Undecylprodigiosin specifically has been shown to have potent anticancer activity against five cancer lines *in vitro* (Liu et al., 2005).

Cell density or biomass dependent regulation for the production of RED2 and RED3 explains the observations from the present study. Cultures of REDMBK6 grown in Russian yeast media began to produce compounds after 3 days of growth, regardless of whether whole yeast was present, because the cultures were dense. After three days in Russian yeast media, spheres of red colored mycelia were clearly visible, and *Streptomyces* began to collect on the edges of the flask. In transfer media, REDMBK6 did not achieve high cell density; cell growth was only discernible as the media clouded.

Whole yeast cells were required in transfer media cultivations to add sufficient cell density and activate production of the RED compounds. It's reasonable to conclude that a physical interaction between REDMBK6 and the yeast was necessary for production in transfer media, since yeast extract did not elicit production of any compounds (Figure 13). Only the presence of additional biomass from a microbial competitor caused production of the RED compounds in transfer media.

Biomass correlated production of prodigiosins has been previously described. Production begins late during culturing and compounds accumulate during the stationary phase of growth when cell mass is greatest. Low culture biomass correlates with lower compound yields (Stankovic et a., 2012). An undecylprodigiosin producing strain in which the cell division factor was over-expressed showed a 20 to 50 fold increase in production of the compound in a fermentor (van Wezel et al., 2006).

Co-culture conditions have also been previously used to increase prodigiosin production in *Streptomyces*. *S. lividans* monocultures produced the red compounds after 3 days of culture and product concentrations increased until day 9 of cultivation. Four times more undecylprodigiosin was produced when *S. lividans* was co-cultured with *Verticillium dahliae,* but the authors did not report the time when production began in co-cultures. In addition, *V. dahliae* is a fungal pathogen that affects the roots of plants and causes vascular wilt world-wide. *S. lividans* significantly reduces the presence of the pathogen when introduced to plant roots infected with *V. dahliae.* The red compounds produced by *S. lividans* collected on and within the fungal hyphae, which subsequently withered. Undecylprodigiosin was the main product in the co-cultures. (Meschke et al., 2012) The production of prodigiosins has also been enhanced in *S. coelicolor* via the addition of sub-inhibitory concentrations of antibiotics to liquid culture (Wang et al., 2014). The *Streptomyces* begin to produce secondary metabolites when compounds from a competing species are detected.

Production of prodigiosins is regulated by the SARP family of regulators, which are growth-phase dependent. When cell density reaches a threshold and the regulatory pathway is activated, there is little downstream control. Production continues as long as precursors are available. (Narva & Feitelson 1989; Barka et al., 2016) A gene encoding a SARP family regulatory was identified with a standard protein BLAST on the regulatory genes identified by AntiSMASH (Figure 27) (Camacho et al., 2009; Blin et al., 2017).

The production of prodigiosins in *Streptomyces* REDMBK6 is correlated with high cell culture density. The results indicate that it is not important whether the threshold cell density is achieved by *Streptomyces* growth or by adding autoclaved whole yeast cells to a culture with low cell density. Further investigation is required to determine whether the autoclaved yeast activates prodigiosin production because it adds biomass to culture, or because it is chemically detected by the *Streptomyces.*

5.2 Production of Polyenes in Co-Culture Conditions

5.2.1 Whole Yeast Cells Elicit Polyene Production

The interaction between *Streptomyces* and fungi was exploited to incite the production of compounds from silent BGCs in well studied strains. Multiple unidentified polyene macrolides were produced by culturing three strains of *Streptomyces* with intact, autoclaved yeast cells. The strains were selected from the in house strain collection because they each have a t1PKS gene cluster that contains a cholesterol oxidase gene. All reported small-sized polyene macrolide gene clusters contain a cholesterol oxidase that functions as a fungal sensor and positive regulator (Aparicio et al., 2016).

The small-sized polyene natamycin, or pimaricin, is not produced when the cholesterol oxidase gene is knocked out, but production is restored by adding cholesterol oxidase enzyme to *Streptomyces* culture. Sterols were discarded as a substrate that cholesterol

oxidase acts on in the natamycin signal transduction pathway. An unknown molecule is used to detect fungi and elicit production of natamycin (Mendes et al., 2007). Results from the current work suggest that the regulation in the tested strains is dependent on a physical interaction with the yeast cell membrane, as yeast extract did not elicit production of the polyenes (Figures 29–31).

5.2.2 HPLC Analysis of Polyene Extracts

HPLC analysis of crude extracts from cultures with comparable biomass show that significantly more compounds were produced when whole yeast was used as the nitrogen source. Each strain had at least one major compound accompanied by several minor peaks with varying retention times that were only present in cultures growth with whole yeast cells (Figures 29–31). The uv/vis spectrum of each co-culture product in all of the strains had three maxima, the most intense of which were 338 nm and 358 nm (Figure 32). The minor peaks are likely intermediate metabolites from various points of the biosynthesis of the final products because they also had uv/vis maxima of 338 nm and 358nm.

The uv/vis spectra of polyene macrolides are dictated by the length and degree of conjugation in the chromophore region. Pentaenes, such as filipin, have three uv/vis maxima between 300nm and 400nm. The maxima shift to longer wavelengths in polyenes with a greater degree of conjugation in the chromophore. (Thomas 1976) The chromophore is synthesized before the macrolactone ring is closed and before subsequent oxidation and glycosylation reactions yield the final compound (Kong et al., 2013). Chemical modifications in the final biosynthetic steps of the compounds would impact retention times with the C18 HPLC column employed, but the finishing steps would not influence the spectra. Therefore, the multiple minor peaks with identical uv/vis spectra are likely biosynthetic intermediates of the major polyene products.

5.2.3 LC-MS Analysis of Crude Extracts

LC-MS results revealed that each of the tested strains produces compounds that have masses between 536 g/mol and 667 g/mol when grown with whole yeast cells. This range is expected of small-sized polyenes whose BGCs contain a cholesterol oxidase encoding gene (Figures 33–36); cholesterol oxidase positively regulates polyene production in the presence of fungi (Aparicio & Martin, 2008). The BGCs for tetramycin and natamycin each contain a cholesterol oxidase, and the masses of these compounds are 695.8 g/mol and 665.7 g/mol, respectively (Cao et al., 2012).

The major product from JCM 4712 with a mass of 667 g/mol could be natamycin (Paseiro-Cerrato et al., 2013). One of the other major products from JCM 4712 could be part of the filipin complex (636 g/mol) (Payero et al., 2015). The compound with mass 536 g/mol produced by JCM 4712 is likely part of the biosynthetic pathway of a major polyene product. This compound is only present in cultivations where polyenes are produced (Figure 36). None of the aforementioned masses were present in extracts from yeast cells.

BKMA 840 and ATCC 27952 produced filipin type compounds. Two of the major compounds produced by BKMA 840 had masses of 636 g/mol and 652 g/mol (Figure 35). These compounds are each 2 mass units less than filipin II and filipin III, respectively. The filipin complex is composed of four different molecules, of which filipin II and filipin III are the major compounds. A loss of two mass units could be caused by the presence of an additional carbon—carbon bond. A compound with mass of 622 g/mol was identified in ATCC 27952. This mass corresponds to filipin I (622 g/mol), which is a precursor to filipin III (654 g/mol) that has two fewer hydroxyl groups (Payero et al., 2015). The exact masses and identities of the discovered compounds cannot be certain, since they were not analyzed with high resolution MS.

In addition to small-sized polyenes, the strains produced other metabolites when grown with yeast. Larger masses were not anticipated, as the BGCs for large polyenes, those with masses over 800 g/mol, have not been reported to contain cholesterol oxidase. However, BKMA 840 had a major product with a mass of 1020 g/mol which was only produced when yeast was present in the culture. Because the production of this compound was associated with the presence of yeast, it is suspected to be an antifungal compound. No known polyenes with this mass could be found. ATCC 27952 produced a compound with a mass of 926 g/mol. The product from ATCC 27952 could be natamycin, which has a mass of 926.1 g/mol (Thomas 1976).

6 Conclusions:

Streptomyces have an extensive secondary metabolism and complex regulatory network to effectively control the production of antimicrobial compounds critical for interspecies competition. It has become increasingly common to use co-culturing conditions to take advantage of the microbial interactions that naturally invoke expression of BGCs (Netzker et al., 2018). The current work has demonstrated that co-culturing *Streptomyces* with *S. cerevisiae* can activate the production of polyene macrolides in strains of *Streptomyces* that do not otherwise produce the compounds. The strains ATCC 27952, BKMA 840 and JCM 4712 were selected based on genome mining of the in house strain collection for t1PKS clusters containing genes that encode cholesterol oxidase. REDMBK6 was selected because it was observed that culturing it with *S. cerevisiae* in transfer media elicited production of red compounds absent in monoculture conditions.

The three *Streptomyces* strains selected based on genetic information all produced compounds hypothesized to be small-sized polyene macrolides based on spectral and mass data, as well as observed antifungal activity. Further work producing and purifying the compounds for NMR is required to definitively identify the products from the co-cultures of *Streptomyces* and *S. cerevisiae*.

The compounds produced by REDMBK6 when grown with yeast were identified as members of the prodigiosin family of compounds. The production of these compounds has been previously shown to be dependent on cell density and enhanced by the presence of competing fungi or sub-inhibitory concentrations of antibiotics (Meschek et al., 2012; Wang et al., 2014).

Strain of *Streptomyces* may contain as many as 50 BGCs, each of which is capable of producing a natural product with potential clinical applications. A majority of the gene

clusters are unexpressed under the nutrient-rich, monoculture conditions, which have been the standard approach for compound discovery (Barka et al., 2016). As a result, the discovery of novel compounds has dramatically slowed in recent decades. A diversity of strategies for the discovery of novel compounds is required if clinical drugs are to remain effective against antibiotic resistant bacteria. Guided approaches utilizing genome mining and microbial-cross talk are becoming increasingly common and could bring about a second golden-age of compound discovery (Stubbendieck & Straight, 2016; Netzker et al., 2018).

Acknowledgements

I would like to thank Prof. Mikko Metsä-Ketelä for providing me the opportunity to join the ABE group and work with such a talented and enjoyable group of people. I consider myself fortunate to have been a part of ABE during my short time in Finland. I want to thank my thesis supervisor Dr. Vilja Siitonen for her endless support, tireless patience and superb sense of humor. Her guidance has been critical to this project and to my growth as a biochemist. I thank my colleagues in ABE for all the laughs and good times we have shared alongside our attempts to tame the fickle *Streptomyces*. Finally, I want to thank all of my friends and family for the encouragement to get through this thesis. I couldn't have done this without the love and support that I have been shown.

Literature

Anderson, T. M., Clay, M. C., Cioffi, A. G., Diaz, K. A., Hisao, G. S., Tuttle, M. D., Nieuwkoop, A. J., Comellas, G., Maryum, N., Wang, S., Uno, B. E., Wildeman, E. L., Gonen, T., Rienstra, C. M., & Burke, M. D. (2014). Amphotericin forms an extramembranous and fungicidal sterol sponge. Nature Chemical Biology, 10(5), 400–406.

Antón, N., Mendes, M. V, Martín, J. F., & Jesús, F. (2004). Identification of PimR as a Positive Regulator of Pimaricin Biosynthesis in Streptomyces natalensis Identification of PimR as a Positive Regulator of Pimaricin Biosynthesis in Streptomyces natalensis. Journal of Bacteriology, 186(9), 2567–2575.

Aparicio, J. F., Caffrey, P., Gil, J. A., & Zotchev, S. B. (2003). Polyene antibiotic biosynthesis gene clusters. Applied Microbiology and Biotechnology, 61(3), 179–188.

Aparicio, J. F., & Martín, J. F. (2008). Microbial cholesterol oxidases: bioconversion enzymes or signal proteins? Molecular BioSystems, 4(8), 804–809.

Aparicio, J. F., Barreales, E. G., Payero, T. D., Vicente, C. M., de Pedro, A., & Santos-Aberturas, J. (2016). Biotechnological production and application of the antibiotic pimaricin : biosynthesis and its regulation. Applied Microbiology and Biotechnology, 100(61), 61–78.

Aszalos, A., Bax, A., Burlinson, N., Roller, P., & McNeal, C. (1985). Physico-chemical and microbiological comparison of nystatin, amphotericin A and amphotericin B, and structure of amphotericin A. The Journal of Antibiotics, 38(12), 1699–1713.

Bachmann, B. O., Van Lanen, S. G., & Baltz, R. H. (2014). Microbial genome mining for accelerated natural products discovery: is a renaissance in the making? Journal of Industrial Microbiology and Biotechnology, 41(2), 175–184.

Baginski, M., Resat, H., & Borowski, E. (2002). Comparative molecular dynamics simulations of amphotericin B – cholesterol/ergosterol membrane channels, Biochimica et Biophysica Acta, 1567, 63–78.

Baginski, M., Sternal, K., Czub, J., & Borowski, E. (2005). Molecular modelling of membrane activity of amphotericin B, a polyene macrolide antifungal antibiotic. Acta Biochimica Polonica, 52(3), 655–658.

Barka, E. A., Vatsa, P., Sanchez, L., Gaveau-Vaillant, N., Jacquard, C., Klenk, H.-P., Clement, C., Ouhdouch, Y., & van Wezel, G. P. (2016). Taxonomy, Physiology, and Natural Products of Actinobacteria. Microbiology and Molecular Biology Reviews, 80(1), 1–43.

Bentley, S. D., Chater, K. F., Cerdeno-Tarrage, A. M., Challis, G. L., Thomson, N. R., James, K. D., Harris, D. E., Quail, M. A., Kieser, H., Harper, D., Bateman, A., Brown, S., Chandra, G., Chen, C. W., Collins, M., Cronin, A., Fraser, A., Goble, A., Hidalgo, J., Hornsby, T., Howarth, S., Huang, C. H., Kieser, T., Larke, L., Murphy, L., Oliver, K., O'Neil, S., Rabbinowitsch, E., M.-A. Rajandream, M. A., Rutherford, K., Rutter, S., Seeger, K., Saunders, D., Sharp, S., Squares, R., Squares, S., Taylor, K., Warren, T., Wietzorrek, A., Woodward, J., Barrell, B. G., Parkhill, J., & Hopwood, D. A., (2002). Complete genome sequence of the model actinomycete Streptomyces. Nature, 417(6885), 141–147.

Blin, K., Wolf, T., Chevrette, M. G., Lu, X., Schwalen, C. J., Kautsar, S. A., Suarez Duran, H. G., de Los Santos, E., Kim, H. U., Nave, M., Dickschat, J. S., Mitchell, D. A.,

Shelest, E., Breitling, R., Takano, E., Lee, S. Y., Weber, T., & Medema, M. H. (2017). antiSMASH 4.0-improvements in chemistry prediction and gene cluster boundary identification. Nucleic acids research, 45(W1), W36-W41.

Burger, K. N. J. (2000). Greasing membrane fusion and fission machineries. Traffic, 1(8), 605–613.

Caffrey, P., Aparicio, J. F., Malpartida, F., & Zotchev, S. B. (2008). Biosynthetic engineering of polyene macrolides towards generation of improved antifungal and antiparasitic agents. Current Topics in Medicinal Chemistry, 8(8), 639–53.

Caffrey, P., De Poire, E., Sheehan, J., & Sweeney, P. (2016). Polyene macrolide biosynthesis in streptomycetes and related bacteria: recent advances from genome sequencing and experimental studies. Applied Microbiology and Biotechnology, 100(9), 3893–3908.

Camacho, C., Coulouris, G., Avagyan, V., Ma, N., Papadopoulos, J., Bealer, K., & Madden, T. L. (2009). BLAST+: architecture and applications. BMC Bioinformatics, 10(421), 1—9.

Cannon, R. D., Lamping, E., Holmes, A. R., Niimi, K., Tanabe, K., Niimi, M., & Monk, B. C. (2007). Candida albicans drug resistance - Another way to cope with stress. Microbiology, 153(10), 3211–3217.

Cao, B., Yao, F., Zheng, X., Cui, D., Shao, Y., Zhu, C., Deng, Z. & You, D. (2012). Genome Mining of the Biosynthetic Gene Cluster of the Polyene Macrolide Antibiotic Tetramycin and Characterization of a P450 Monooxygenase Involved in the Hydroxylation of the Tetramycin B Polyol Segment. ChemBioChem, 13(15), 2234–2242.

Carver, T., Harris, S. R., Berriman, M., Parkhill, J., McQuillan, J. A. (2012). Artemis: an integrated platform for visualization and analysis of high-throughput sequence-based experimental data. Bioinformatics, 28(4), 464-469.

Challis, G. L. (2014). Exploitation of the Streptomyces coelicolor A3(2) genome sequence for discovery of new natural products and biosynthetic pathways. Journal of Industrial Microbiology & Biotechnology, 41(2), 219–232.

Chen, W. C., Chou, D. L., & Feingold, D. S. (1978). Dissociation between ion permeability and the lethal action of polyene antibiotics on Candida albicans. Antimicrobial Agents and Chemotherapy, 13(6), 914–917.

Chudzik, B., Koselski, M., Czuryło, A., Trębacz, K., & Gagoś, M. (2015). A new look at the antibiotic amphotericin B effect on Candida albicans plasma membrane permeability and cell viability functions. European Biophysics Journal, 44(1–2), 77–90.

Ciesielski, F., Griffin, D. C., Loraine, J., Rittig, M., Delves-Broughton, J., & Bonev, B. B. (2016). Recognition of Membrane Sterols by Polyene Antifungals Amphotericin B and Natamycin, A 13C MAS NMR Study. Frontiers in Cell and Developmental Biology, 4(57), 1–12.

Cohen, B. E. (2010). Amphotericin B membrane action: Role for two types of ion channels in eliciting cell survival and lethal effects. Journal of Membrane Biology, 238(1–3), 1–20.

Dalhoff, A. A. H., & Levy, S. B. (2015). Does use of the polyene natamycin as a food preservative jeopardise the clinical efficacy of amphotericin B? A word of concern. International Journal of Antimicrobial Agents, 45(6), 564–567

Delattin, N., Cammue, B. P., & Thevissen, K. (2014). Reactive oxygen species-inducing antifungal agents and their activity against fungal biofilms. Future Medicinal Chemistry, 6(1), 77–90.

Falk, R., Domb, A. J., & Polacheck, I. (1999). A novel injectable water-soluble amphotericin B-arabinogalactan conjugate. Antimicrobial Agents and Chemotherapy, 43(8), 1975–1981.

Gary-Bobo, C. M. (1989). Polyene-sterol interaction and selective toxicity. Biochimie, 71(1), 37–47.

Ghannoum, M. A., & Rice, L. B. (1999). Antifungal agents: mode of action, mechanisms of resistance, and correlation of these mechanisms with bacterial resistance. Clinical Microbiology Reviews, 12(4), 501–517.

Gray, K. C., Palacios, D. S., Dailey, I., Endo, M. M., Uno, B. E., Wilcock, B. C., & Burke, M. D. (2012). Amphotericin primarily kills yeast by simply binding ergosterol. Proceedings of the National Academy of Sciences, 109(7), 2234–2239.

Gupte, M., Kulkarni, P., & Ganguli, B. N. (2002). Antifungal antibiotics. Applied Microbiology and Biotechnology, 58(1), 46–57.

Hamill, R. J. (2013). Amphotericin B formulations: A comparative review of efficacy and toxicity. Drugs, 73(9), 919–934.

Hartsel, S. C., Hatch, C., & Ayenew, W. (1993). How does AmB work?: studies on model membrane systems. J. Liposome Res., 3(3), 377–408.

Hazen, E., & Brown, R. (1950). Fungicidin, an Antibiotic Produced by a Soil Actinomycetes. R.F. Science, 112(423), 93–97.

Hopwood, D. A. (1997). Genetic Contributions to Understanding Polyketide Synthases. Chemical Reviews, 97(7), 2465–2498.

Ibrahim, O. (2013). Studies Towards the Efficient Isolation and Purification of Analogues of Amphotericin B from Streptomyces. University of Leicester, Department of Chemistry, Doctor of Philosophy Thesis.

Janout, V., Schell, W. A., Thévenin, D., Yu, Y., Perfect, J. R., & Regen, S. L. (2015). Taming Amphotericin B. Bioconjugate Chemistry, 26(10), 2021–2024.

Johnson, R., Ho, J., Fowler, P., & Heidari, A. (2018). Coccidioidal Meningitis: A Review on Diagnosis, Treatment, and Management of Complications. Current Neurology and Neuroscience Reports, 18(4), 1–8.

Kamiński, D. M., Czernel, G., Murphy, B., Runge, B., Magnussen, O. M., & Gagoś, M. (2014). Effect of cholesterol and ergosterol on the antibiotic amphotericin B interactions with dipalmitoylphosphatidylcholine monolayers: X-ray reflectivity study. Biochimica et Biophysica Acta - Biomembranes, 1838(11), 2947–2953.

Kong, D., Lee, M. J., Lin, S., & Kim, E. S. (2013). Biosynthesis and pathway engineering of antifungal polyene macrolides in actinomycetes. Journal of Industrial Microbiology and Biotechnology, 40(6), 529–543.

Lemke, A., Kiderlen, A. F., & Kayser, O. (2005). Amphotericin B. Applied Microbiology and Biotechnology, 68(1), 151–162.

Lewis, K. (2013). Platforms for antibiotic discovery. Nature Reviews Drug Discovery, 12(5), 371–387.

Liu, G., Chater, K. F., Chandra, G., Niu, G., & Tan, H. (2013). Molecular Regulation of Antibiotic Biosynthesis in Streptomyces. Microbiology and Molecular Biology Reviews, 77(1), 112–143.

Liu, R., Cui, C.-B., Duan, L., Gu, Q.-Q., & Zhu, W.-M. (2005). Potent in vitro anticancer activity of metacycloprodigiosin and undecylprodigiosin from a sponge-derived actinomycete Saccharopolyspora sp. nov. Archives of Pharmacal Research, 28(12), 1341–1344.

Low, Z. J., Pang, L. M., Ding, Y., Cheang, Q. W., Hoang, K. L. M., Tran, H. T., Li, J., Liu, X., Kanagasundaram, Y., & Liang, Z. X. (2018). Identification of a biosynthetic gene cluster for the polyene macrolactam sceliphrolactam in a Streptomyces strain isolated from mangrove sediment. Scientific Reports, 8(1594), 1–11.

Lyu, X., Zhao, C., Hua, H., & Yan, Z. (2016). Efficacy of nystatin for the treatment of oral candidiasis: a systematic review and meta-analysis. Drug Design, Development and Therapy, 10, 1161–1171.

Malayeri, F. A., Rezaei, A. A., & Raiesi, O. (2018). Antifungal agents: Polyene, azole, antimetabolite, other and future agents. J Bas Res Med Sci, 5(2), 48–55.

Medema, M. H., Cimermancic, P., Sali, A., Takano, E., & Fischbach, M. A. (2014). A Systematic Computational Analysis of Biosynthetic Gene Cluster Evolution: Lessons for Engineering Biosynthesis. PLoS Computational Biology, 10(12), 1–12.

Mendes, M. V., Recio, E., Antón, N., Guerra, S. M., Santos-Aberturas, J., Martín, J. F. F., & Aparicio, J. F. (2007). Cholesterol Oxidases Act as Signaling Proteins for the Biosynthesis of the Polyene Macrolide Pimaricin. Chemistry and Biology, 14(3), 279–290.

Mesa-Arango, A. C., Scorzoni, L., & Zaragoza, O. (2012). It only takes one to do many jobs: Amphotericin B as antifungal and immunomodulatory drug. Frontiers in Microbiology, 3(286), 1–10.

Mesa-Arango, A. C., Trevijano-Contador, N., Román, E., Sánchez-Fresneda, R., Casas, C., Herrero, E., Argüelles, J. C., Pla, J., Cuenca-Estrella, M. & Zaragoza, O. (2014). The production of reactive oxygen species is a universal action mechanism of amphotericin B against pathogenic yeasts and contributes to the fungicidal effect of this drug. Antimicrobial Agents and Chemotherapy, 58(11), 6627–6638.

Meschke, H., Walter, S., & Schrempf, H. (2012). Characterization and localization of prodiginines from Streptomyces lividans suppressing Verticillium dahliae in the absence or presence of Arabidopsis thaliana. Environmental Microbiology, 14(4), 940–952.

Mouri, R., Konoki, K., Matsumori, N., Oishi, T., & Murata, M. (2008). Affinity of Amphotericin B to Sterol-Containing Liposomes as Evidenced by Surface Plasmon Resonance. Biochemistry, 47, 7807–7815.

Narva, K. E., & Feitelson, J. S. (1990). Nucleotide sequence and transcriptional analysis of the redD locus of Streptomyces coelicolor A3(2). Journal of Bacteriology, 172(1), 326–333.

Nazari, B., Kobayashi, M., Saito, A., Hassaninasab, A., Miyashita, K., & Fujiia, T. (2013). Chitin-induced gene expression in secondary metabolic pathways of

Streptomyces coelicolor A3(2) grown in soil. Applied and Environmental Microbiology, 79(2), 707–713.

Netzker, T., Flak, M., Krespach, M. K. C., Stroe, M. C., Weber, J., Schroeckh, V., & Brakhage, A. A. (2018). Microbial interactions trigger the production of antibiotics. Current Options in Microbiology, 45, 117–123.

Palacios, D. S., Dailey, I., Siebert, D. M., Wilcock, B. C., & Burke, M. D. (2011). Synthesis-enabled functional group deletions reveal key underpinnings of amphotericin B ion channel and antifungal activities. Proceedings of the National Academy of Sciences of the United States of America, 108(17), 6733–6738.

Paseiro-Cerrato, R., Otero-Pazos, P., Rodriguez-Bernaldo de Quirós, A., Sendón, R., Angulo, I., & Paseiro-Losada, P. (2013). Rapid method to determine natamycin by HPLC-DAD in food samples for compliance with EU food legislation. Food Control, 33(1), 262–267.

Payero, T. D., Vicente, C. M., Rumbero, Á., Barreales, E. G., Santos-Aberturas, J., de Pedro, A., & Aparicio, J. F. (2015). Functional analysis of filipin tailoring genes from Streptomyces filipinensis reveals alternative routes in filipin III biosynthesis and yields bioactive derivatives. Microbial Cell Factories, 14(1), 1–14.

Peters, C., Bayer, M. J., Bühler, S., Andersen, J. S., Mann, M., & Mayer, A. (2001). Trans-complex formation by proteolipid channels in the terminal phase of membrane fusion. Nature, 409(6820), 581–588.

Pfaller, M. A., Espinel-Ingroff, A., Canton, E., Castanheira, M., Cuenca-Estrella, M., Diekema, D. J., Fothergill, A., Fuller, J., Ghannoum, M., Jones, R. N., Lockhart, S. R., Martin-Manzuelos, E., Melhem, M. S. C., Ostrosky-Zeichner, L., Pappas, P., Pelaez, T.,

Peman, J., Rex, J., & Szeszs, M. W. (2012). Wild-type MIC distributions and epidemiological cutoff values for amphotericin B, flucytosine, and itraconazole and Candida spp. as determined by CLSI broth microdilution. Journal of Clinical Microbiology, 50(6), 2040–2046.

Pospiech, A. and Neumann, B. (1995) A versatile quick-prep of genomic DNA from grampositive bacteria. Trends in Genetics, 11, 217–218.

Romero, E. A., Valdivieso, E., & Cohen, B. E. (2009). Formation of two different types of ion channels by amphotericin B in human erythrocyte membranes. Journal of Membrane Biology, 230(2), 69–81.

Sangalli-Leite, F., Scorzoni, L., Mesa-Arango, A. C., Casas, C., Herrero, E., Soares Mendes Gianinni, M. J., Rodriguez-Tudela, J. L., Cuenca-Estrella, M., & Zaragoza, O. (2011). Amphotericin B mediates killing in Cryptococcus neoformans through the induction of a strong oxidative burst. Microbes and Infection, 13(5), 457–467.

Sanglard, D., Ischer, F., Parkinson, T., Bille, J., & Falconer, D. (2003). Candida albicans Mutations in the Ergosterol Biosynthetic Pathway and Resistance to Several Antifungal Agents Candida albicans Mutations in the Ergosterol Biosynthetic Pathway and Resistance to Several Antifungal Agents. Antimicrobial Agents and Chemotherapy, 47(8), 2404–2412.

Santos-Aberturas, J., Engel, J., Dickerhoff, J., Dörr, M., Rudroff, F., Weisz, K., & Bornscheuer, U. T. (2015). Exploration of the substrate promiscuity of biosynthetic tailoring enzymes as a new source of structural diversity for polyene macrolide antifungals. ChemCatChem, 7(3), 490–500.

Scheibler, E., Garcia, M. C. R., Medina da Silva, R., Figueiredo, M. A., Salum, F. G., & Cherubini, K. (2017). Use of nystatin and chlorhexidine in oral medicine: Properties, indications and pitfalls with focus on geriatric patients. Gerodontology, 34(3), 291–298.

Scherlach, K., Graupner, K., & Hertweck, C. (2013). Molecular Bacteria-Fungi Interactions: Effects on Environment, Food, and Medicine. Annual Review of Microbiology, 67(1), 375–397.

Shekhova, E., Kniemeyer, O., & Brakhage, A. A. (2017). Induction of mitochondrial reactive oxygen species production by itraconazole, terbinafine, and amphotericin B as a mode of action against Aspergillus fumigatus. Antimicrobial Agents and Chemotherapy, 61(11), 1–35.

Stankovic, N., Radulovic, V., Petkovic, M., Vuckovic, I., Jadranin, M., Vasiljevic, B., & Nikodinovic-Runic, J. (2012). Streptomyces sp. JS520 produces exceptionally high quantities of undecylprodigiosin with antibacterial, antioxidative, and UV-protective properties. Applied Microbiology and Biotechnology, 96(5), 1217–1231.

Stubbendieck, R. M., & Straight, P. D. (2016). Multifaceted Interfaces of Bacterial Competition. Journal of Bacteriology, 198(16), 2145–55.

Svahn, K. S., Chryssanthou, E., Olsen, B., Bohlin, L., & Göransson, U. (2015). Penicillium nalgiovense Laxa isolated from Antarctica is a new source of the antifungal metabolite amphotericin B. Fungal Biology and Biotechnology, 2(1), 1–8.

Szlinder-Richert, J., Mazerski, J., Cybulska, B., Grzybowska, J., & Borowski, E. (2001). MFAME , N-methyl-N- D -fructosyl amphotericin B methyl ester, a new amphotericin B derivative of low toxicity : relationship between self-association and effects on red blood cells. Biochimica et Biophysica Acta, 1528(2001), 15–24.

Szpilman, A. M., Manthorpe, J. M., & Carreira, E. M. (2008). Synthesis and biological studies of 35-deoxy amphotericin B methyl ester. Angewandte Chemie - International Edition, 47(23), 4339–4342.

Te Welscher, Y. M., Ten Napel, H. H., Balagué, M. M., Souza, C. M., Riezman, H., De Kruijff, B., & Breukink, E. (2008). Natamycin blocks fungal growth by binding specifically to ergosterol without permeabilizing the membrane. Journal of Biological Chemistry, 283(10), 6393–6401.

Te Welscher, Y. M., Jones, L., Leeuwen, M. R. Van, Dijksterhuis, J., Kruijff, B. De, Eitzen, G., & Breukink, E. (2010). Natamycin Inhibits Vacuole Fusion at the Priming Phase via a Specific Interaction with Ergosterol. Antimicrobial Agents and Chemotherapy, 54(6), 2618–2625.

Te Welscher, Y. M., van Leeuwen, M. R., De Kruijff, B., Dijksterhuis, J., & Breukink, E. (2012). Polyene antibiotic that inhibits membrane transport proteins. Proceedings of the National Academy of Sciences of the United States of America, 109(28), 11156–11159.

Thomas, A. H. (1976). The Analyst Analysis and Assay of Polyene Antifungal Antibiotics A Review Summary of Contents Introduction Chemical and Biological Properties Production Chemical Methods of Analysis and Assay Biological Assay Stability Conclusions, 101(1202), 321–340.

Traxler, M. F., & Kolter, R. (2015). Natural products in soil microbe interactions and evolution. Nat. Prod. Rep., 32(7), 956–970.

Tutaj, K., Szlazak, R., Starzyk, J., Wasko, P., Grudzinski, W., Gruszecki, W. I., & Luchowski, R. (2015). Journal of Photochemistry and Photobiology B : Biology The

orientation of the transition dipole moments of a polyene antibiotic Amphotericin B under UV – VIS studies. Journal of Photochemistry & Photobiology, B: Biology, 151(2015), 83–88.

Umegawa, Y., Nakagawa, Y., Tahara, K., Tsuchikawa, H., Matsumori, N., Oishi, T., & Murata, M. (2012). Head-to-tail interaction between amphotericin b and ergosterol occurs in hydrated phospholipid membrane. Biochemistry, 51(1), 83–89.

van Arnam, E. B., Ruzzini, A. C., Sit, C. S., Horn, H., Pinto-Tomás, A. A., Currie, C. R., & Clardy, J. (2016). Selvamicin, an atypical antifungal polyene from two alternative genomic contexts. Proceedings of the National Academy of Sciences, 113(46), 12940–12945.

van der Meij, A., Worsley, S. F., Hutchings, M. I., & van Wezel, G. P. (2017). Chemical ecology of antibiotic production by actinomycetes. FEMS Microbiology Reviews, 41(3), 392–416. https://doi.org/10.1093/femsre/fux005

van Wezel, G. P., Krabben, P., Traag, B. A., Keijser, B. J. F., Kerste, R., Vijgenboom, E., Heijnen, J. J., & Kraal, B. (2006). Unlocking Streptomyces spp. for use as sustainable industrial production platforms by morphological engineering. Applied and Environmental Microbiology, 72(8), 5283–5288.

van Wezel, G. P., & McDowall, K. J. (2011). The regulation of the secondary metabolism of Streptomyces: new links and experimental advances. Natural Product Reports, 28(1), 1311–1333.

Vincent, B. M., Lancaster, A. K., Scherz-Shouval, R., Whitesell, L., & Lindquist, S. (2013). Fitness Trade-offs Restrict the Evolution of Resistance to Amphotericin B. PLoS Biology, 11(10), 1–17.

Walker, L. A., Gow, N. A. R., & Munro, C. A. (2010). Fungal echinocandin resistance. Fungal Genetics and Biology, 47(2), 117–126.

Wang, H., He, X., Sun, C., Gao, J., Liu, X., & Liu, H. (2018). Enhanced natamycin production by co-expression of Vitreoscilla hemoglobin and antibiotic positive regulators in Streptomyces gilvosporeus. Biotechnology & Biotechnological Equipment, 2818, 1–7.

Wang, W., Ji, J., Li, X., Wang, J., Li, S., Pan, G., Fan, K, & Yang, K. (2014). Angucyclines as signals modulate the behaviors of Streptomyces coelicolor. Proceedings of the National Academy of Sciences, 111(15), 5688–5693.

Wasko, P., Luchowski, R., Tutaj, K., Grudzinski, W., Adamkiewicz, P., & Gruszecki, W. I. (2012). Toward Understanding of Toxic Side Effects of a Polyene Antibiotic Amphotericin B: Fluorescence Spectroscopy Reveals Widespread Formation of the Specific Supramolecular Structures of the Drug. Molecular Pharmaceutics, 9(1), 1511-1520.

Zhou, Y., Liao, M., Zhu, C., Hu, Y., Tong, T., Peng, X., Li, M., Feng, M., Cheng, L., Ren, B. & Zhou, X. (2018). ERG3 and ERG11 genes are critical for the pathogenesis of Candida albicans during the oral mucosal infection. International Journal of Oral Science, 10(2), 1–8.

Zotchev, S. B. (2003). Polyene macrolide antibiotics and their applications in human therapy. Current Medicinal Chemistry, 10(3), 211–23.